Electronic Supplementary Information – New Journal of Chemistry

Palladium(II) complexes bearing 1-iminothiolate-3,5-dimethylpyrazoles: synthesis, cytotoxicity, DNA binding and enzymatic inhibition studies

Thales Reggiani de Moura,*[a] Renan Diego Zanetti,[a] Debora Eduarda Soares Silva,[a] Renan Lira Farias,[a] Antonio Eduardo Mauro,[a] José Clayston Melo Pereira,[a] Aline Aparecida de Souza,[b] Fábio da Silva Siqueira,[b] Wagner Alves de Souza Júdice,[b] Mauro Almeida Lima,[c] Fillipe Vieira Rocha,[c] Victor Marcelo Deflon[d] and Adelino Vieira de Godoy Netto[a]

[a.] UNESP – Univ Estadual Paulista, Instituto de Química, Departamento de Química Geral e Inorgânica, 14800-060, Araraquara, SP, Brazil
[b.] UMC –Univ de Mogi das Cruzes, Centro Interdisciplinar de Investigação Bioquímica, 08701-970, Mogi das Cruzes, SP, Brazil.
[c.] UFSCar – Univ Federal de São Carlos, Departamento de Química, 13565-905, São Carlos, SP, Brazil
[d.] USP – Univ de São Paulo, Instituto de Química de São Carlos, 13560-970, São Carlos, SP, Brazil

*Corresponding author: e-mail address. thalesreggiani@gmail.com
tel. +55 17 98122-8137

S1. Experimental Methods:

S1.1. X-ray crystallography

The crystal structure (Fig. 1) was elucidated by X-ray single crystal diffraction at room temperature (CCDC number: 2006687). Data collections for single crystal structure determination of **3** were performed on a BRUKER KAPPA APEX II DUO diffractometer using graphite-monochromated MoKα radiation (λ = 0.71073 Å) at 23°C. The multi-scan absorption correction method was employed. SHELXS and SHELXL software were used for structure solution and refinement.[1] The hydrogen atoms positions were refined with fixed individual isotropic displacement parameters using a riding model. All non-hydrogen atoms positions were refined with anisotropic thermal displacements. A summary of the crystal data, experimental details and refinement results is given in Table 1S.

Table 1S.1 Crystal and structure refinement data for cis-[PdCl(N,S-**L_3**)(PPh_3)] (**3**)

Formula	$C_{26}H_{27}ClN_3PPdS$
Formula weight	586.38
Wavelength	0.71073 Å
Crystal system	Orthorhombic
Space group	P b c a
Temperature /K	296(2) K
a / Å	9.1066(3) Å α= 90°
b / Å	14.6728(5) Å β= 90°
c / Å	38.6322(14) Å γ = 90°
V /Å^3	5162.0(3) Å^3
Z	8
D_{calc}	1.509 Mg/m^3
Absorption coefficient	0.985 mm^{-1}
F(000)	2384
Crystal size	0.880 x 0.380 x 0.200 mm^3
ϑ range for data collection (°)	2.109 to 26.395°.
Index ranges	-11<=h<=11, -18<=k<=18, -48<=l<=48
Reflections collected	77198
Independent reflections	5292 [R(int) = 0.0287]
Completeness to theta = 25.242°	100.0 %
Absorption correction	Semi-empirical from equivalents
Max. and min. transmission	0.7454 and 0.5288
Refinement method	Full-matrix least-squares on F^2
Data / restraints / parameters	5292 / 0 / 301
Goodness-of-fit on F^2	1.375
Final R indices [I>2sigma(I)]	R1 = 0.0424, wR2 = 0.1079
R indices (all data)	R1 = 0.0442, wR2 = 0.1090
Largest diff. peak and hole	0.535 and -1.789 e.Å^{-3}

S1.2. DNA interaction studies

A standard solution of calf thymus DNA (CT-DNA) was prepared in Tris–HCl buffer (5 mM Tris–HCl and 50 mM NaCl, pH 7.3). The purity of the DNA solution was verified by the ratio between 260 and 280 nm absorption bands with values in the range of 1.8-1.9 that are consistent with a solution free of proteins. The DNA concentration was determined spectrophotometrically using the molar absorption coefficient of 6600 L mol^{-1} cm^{-1} at 260 nm.[2]

S1.3. Spectroscopic titration

The titration experiments were performed in a quartz cell with Tris-HCl buffer with 2% DMSO and concentration of the complex fixed in 20 µM. The UV-vis spectra were obtained with increasing amounts of CT-DNA with concentration ranging from 0 to 60 µM, that was added both in the compound solution and the reference. The binding constant (K_b) was obtained by the Wolfe-Shimer relationship.[3,4]

Wolfe-Shimer Equation: $\frac{[DNA]}{(\varepsilon_a-\varepsilon_f)} = \frac{[DNA]}{(\varepsilon_b-\varepsilon_f)} + \frac{1}{K_b(\varepsilon_b-\varepsilon_f)}$ *

* *[DNA] is the concentration of CT-DNA, the molar absorptivity coefficients εa, εf and εb correspond to Aobs/[complex], the free compounds and the compounds in the fully bound form, respectively. Kb is the binding constant in M-1. The value of the constant was calculated by the ratio between the slope and the linear coefficient in a plot of [DNA]/ε_a-ε_f versus [DNA].

Complex 2:

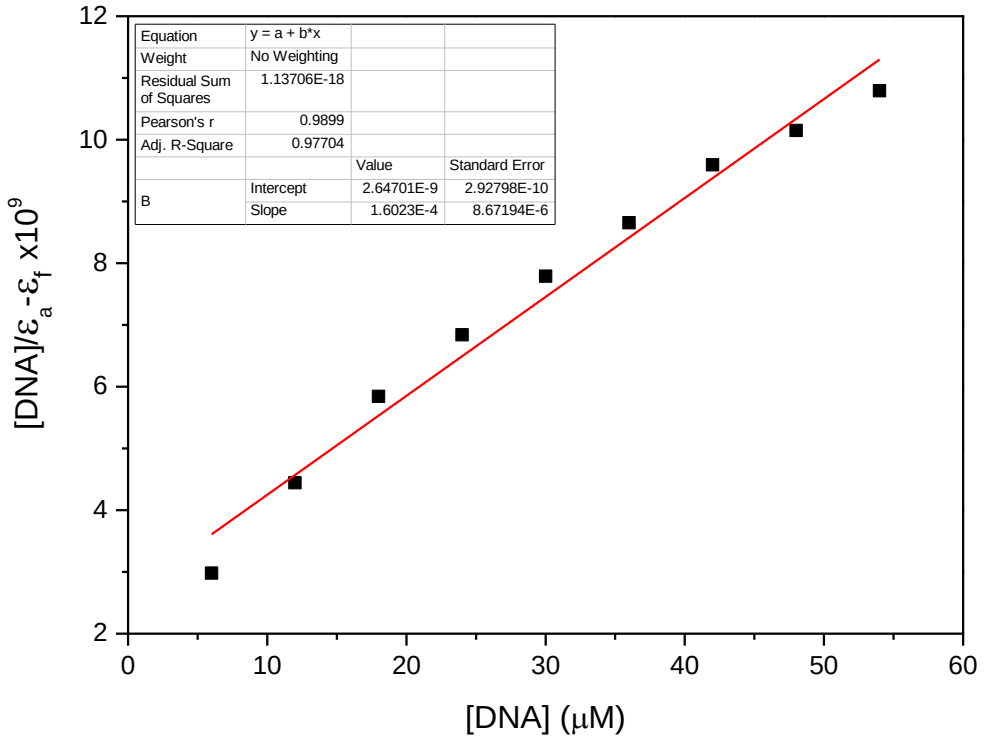

Complex 3:

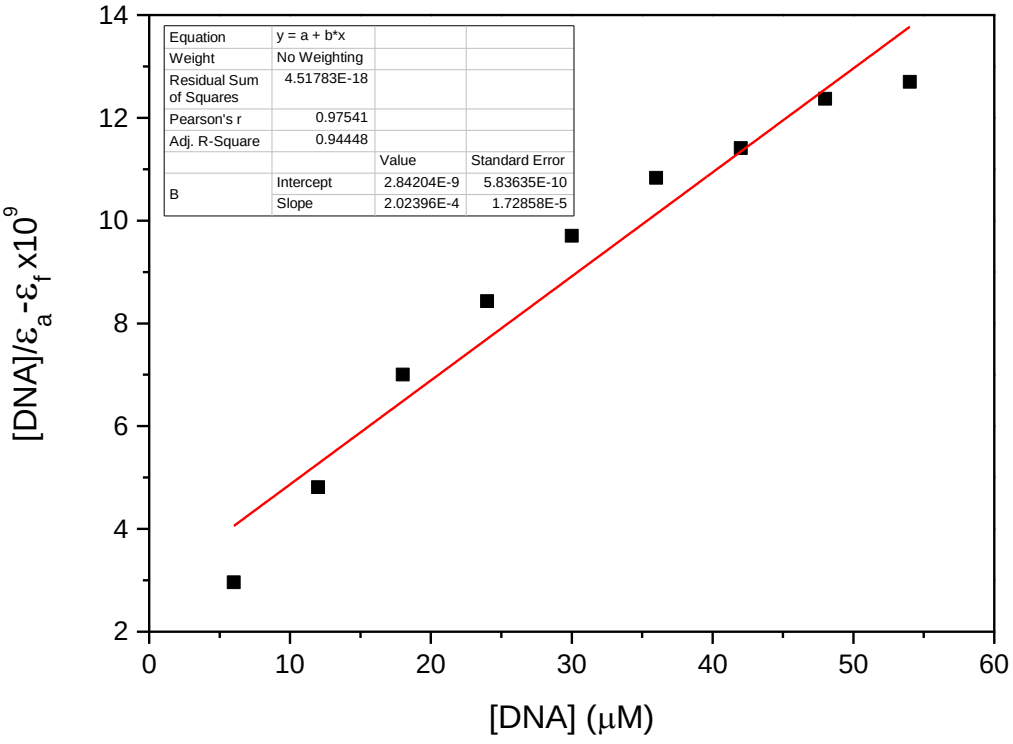

S1.4. Circular dichroism (CD)

The CD spectra were obtained ranging from 235 to 300 nm using a standard quartz cell of 10 mm path length. The spectra were recorded with accumulation of 5 scans in a continuous scanning mode (100 nm/min). The concentration of the DNA solution in Tris-HCl buffer was kept constant in all samples (50 µM). The complex solution was freshly prepared in DMSO (1 mM) and then additions were made to DNA solution to achieve molar ratio of complex/DNA from 0 to 0.3, maintaining DMSO percentage lower than 2%. The samples of pure DNA and DNA-Complex were incubated at 37 °C for 24 h before the CD spectra were collected.[5]

S1.5. Hoechst 33258 Displacement Experiments

The competitive displacement Hoeschst 33258 assay was ranging from 358 to 660 nm, with excitation wavelength of 340 nm and 5.0 nm bandwidth. The DNA and Hoechst 33258 concentrations were kept fixed in 60 µM and 6 µM, respectively. The complex solution freshly prepared in DMSO (2 mM) was added to DNA-Hoechst 33258 solution in order to achieve concentrations from 0 to 54 µM (molar ratios from 0 to 0.9 complex/DNA). The percentage of DMSO in the experiment was maintained lower than 3%. All the spectra were recorded after an interval of 5 min between each addition. To evaluate the affinity of the compounds by the DNA, the Stern-Volmer relationship was applied and the value of the quenching constant (K_{sv}) calculated.[6]

Stern-Volmer Equation: $F_0/F = 1 + K_{SV}[Q]$*

* F0 and F are fluorescence intensity of Hoechst-DNA adduct before and after the compound addition, respectively. The Ksv is the quenching constant of Stern-Volmer and [Q] is the compound concentration. The value of the constant was obtained by the slope of the linear plot of F0/F versus [Q].

Complex 2:

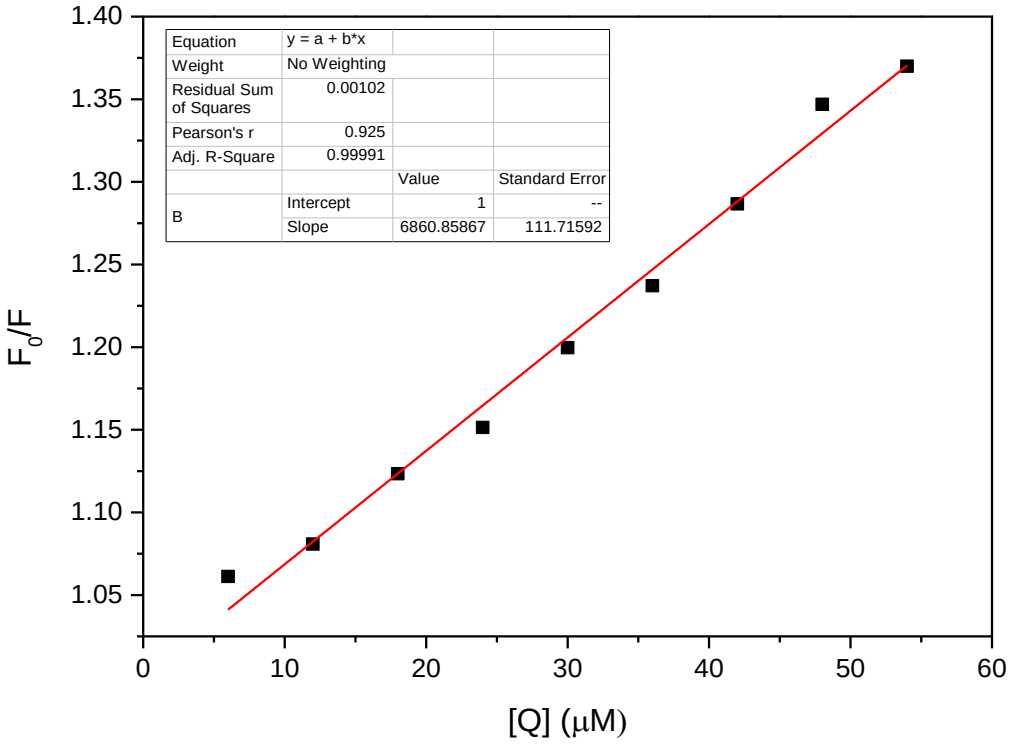

Complex 3:

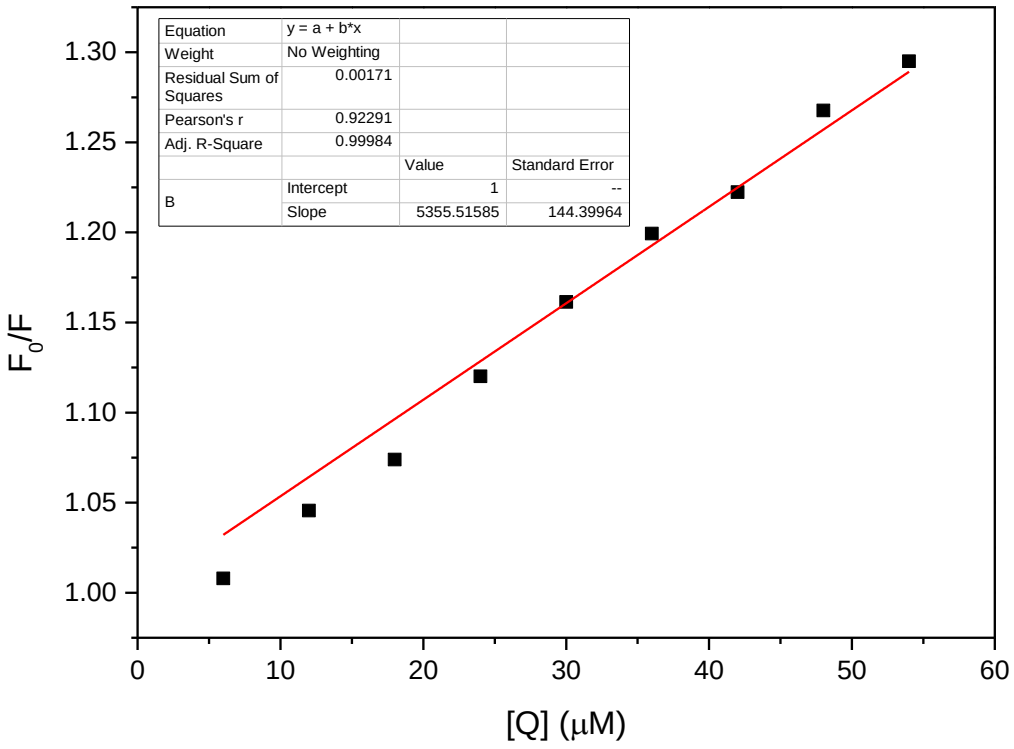

S1.6. Topoisomerase IIα Interaction: Relaxation Assay

The Human Topoisomerase II relaxation kit was purchased from Inspiralis Limited, Norwich, United Kingdom. The reaction mixture (30 µL) contained 10 mmol L^{-1} TrisHCl (pH 7.9), 50 mmol L^{-1} NaCl, 50 mmol L^{-1} KCl, 5.0, mmol L^{-1} $MgCl_2$, 0.1 mmol L^{-1} Na_2H_2EDTA, 15 mg mL^{-1} BSA, 1.0 mmol L^{-1} ATP, 500 ng pBR322 DNA, and 4.0 nmol L^{-1} Topo IIα, with two different concentrations of the complexes. The reaction mixtures were incubated at 37 °C for 1 h. The reaction was terminated by the addition of 3 µL SDS, 15 µL of STEB and 60 µL of chloroform: the isoamyl alcohol (24:1 v/v) mixture was centrifuged and analyzed. The samples were electrophoresed at 30 V for 12 h. The gel was then stained with ethidium bromide solution (1 mg mL^{-1}) and analyzed by the Gel Doc™ EZ Gel.

S1.7. Docking studies and modelling calculation

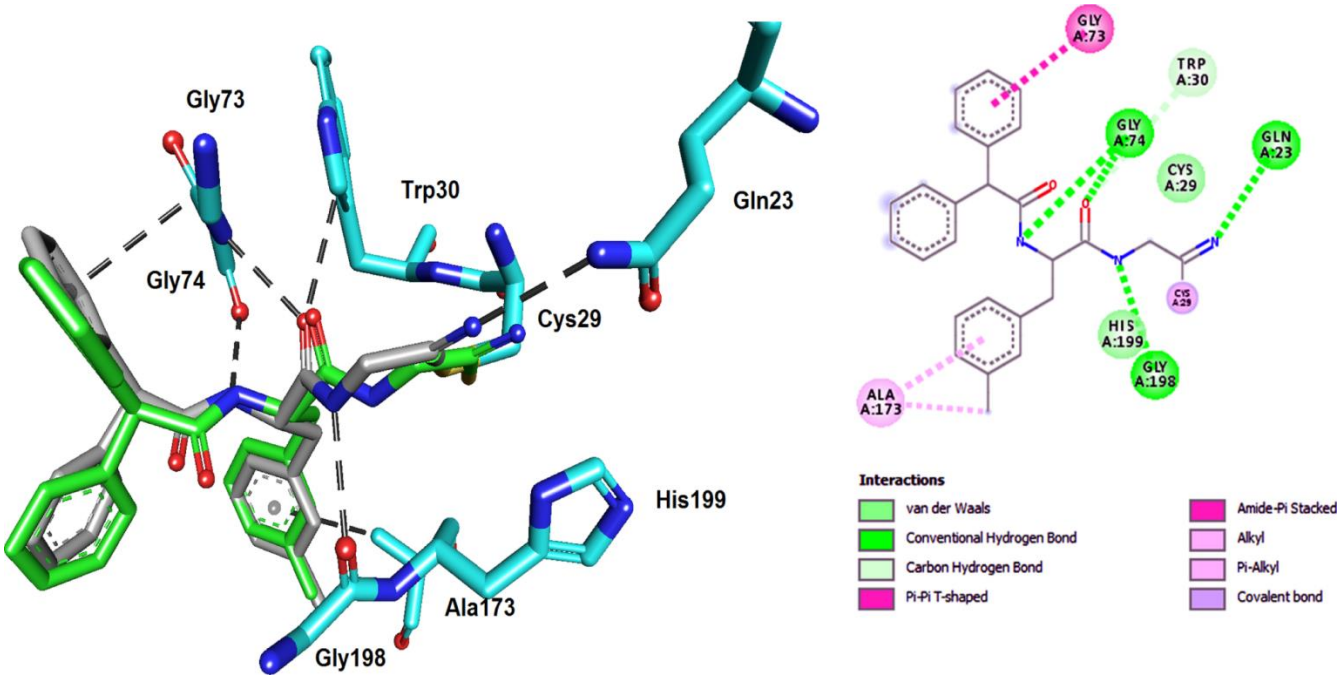

Fig. S1. Left: Redocked dipeptidyl inhibitor (carbons in green) with smallest RMSD 1.673Å superimposed on original crystal structure from 1GMY.pdb. Right: 2-D diagram of key residues and intermolecular contacts in the S-site pocket

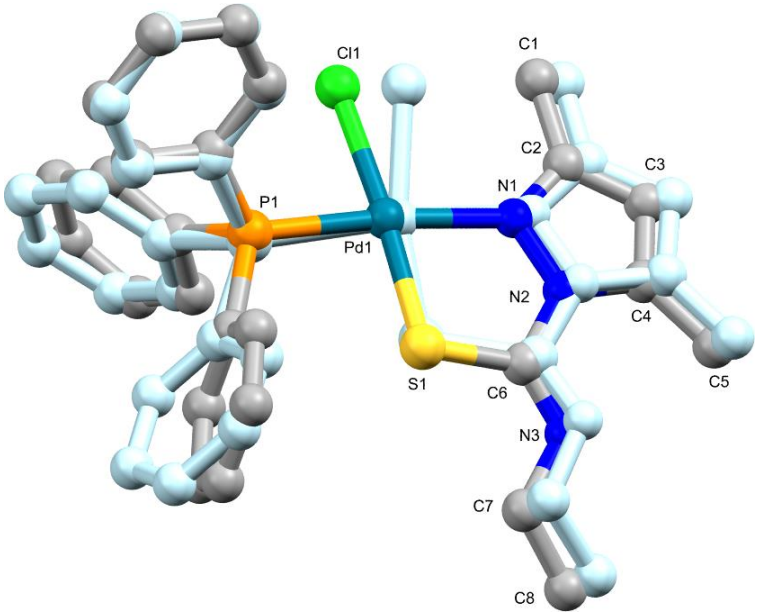

Fig. S2. Heavy atom overlay between the crystallographic and theoretical structures of **3**. The RMSD value amounts to 0.4884 Å. The theoretical result is shown as light blue ball-and-stick representation.

S2. Characterization of ligands and complexes

S2.1. NMR Spectra

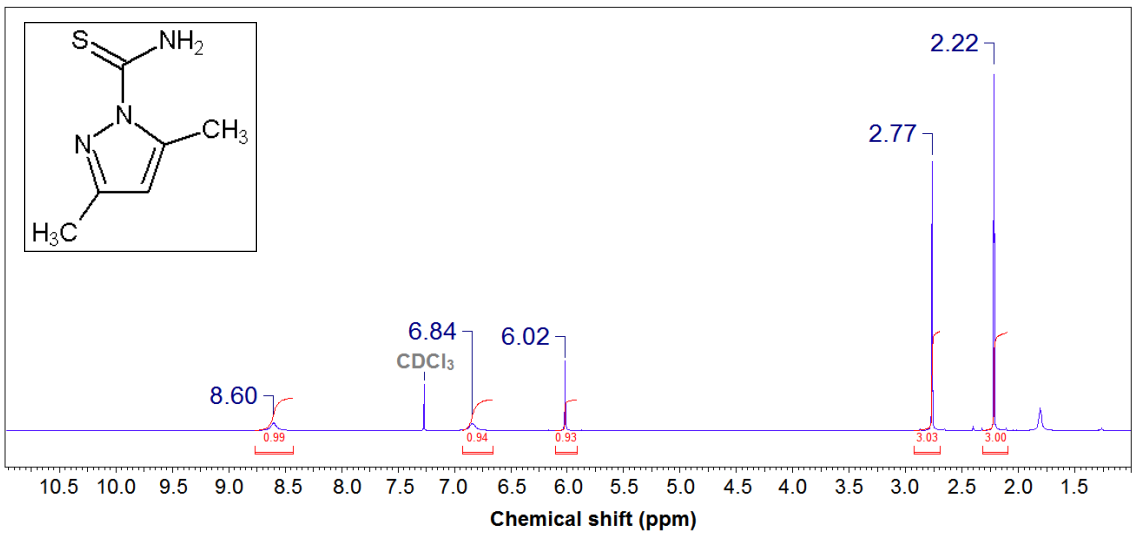

Fig. S3 ^{1}H NMR spectrum of **HL_1**

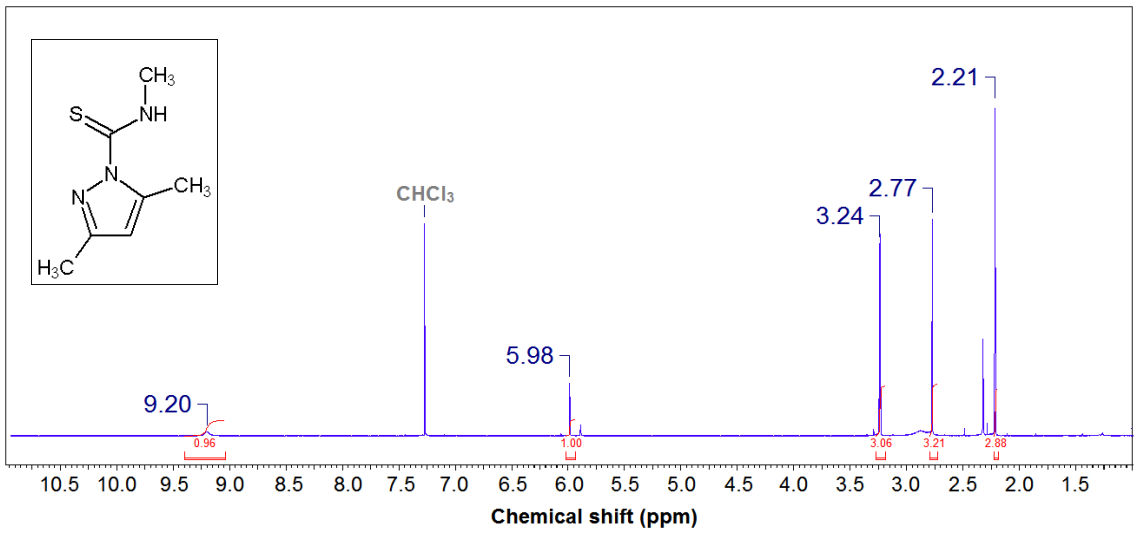

Fig. S4. ^{1}H NMR spectrum of **HL_2**

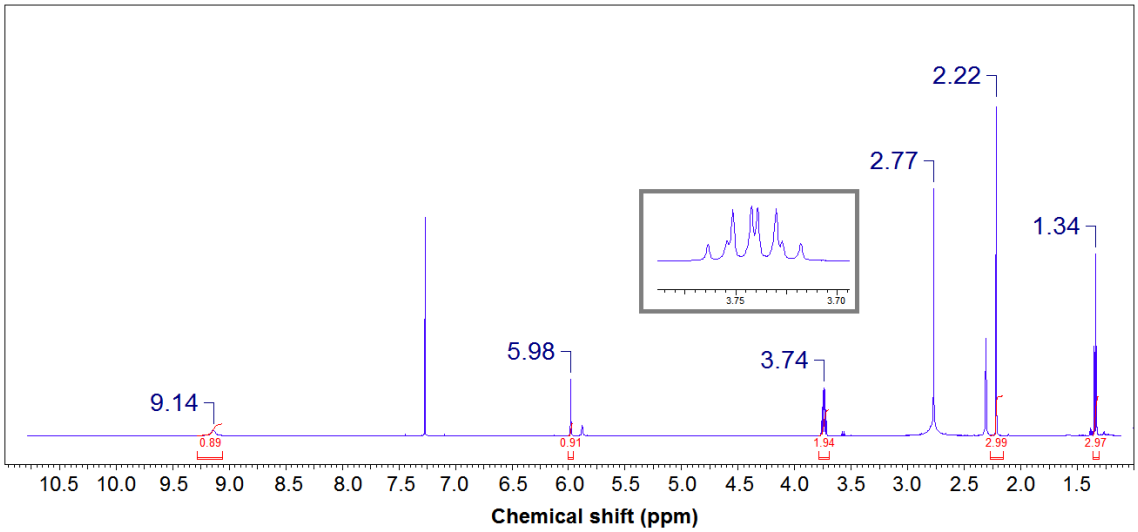

Fig. S5. ^{1}H NMR spectrum of **HL_3**

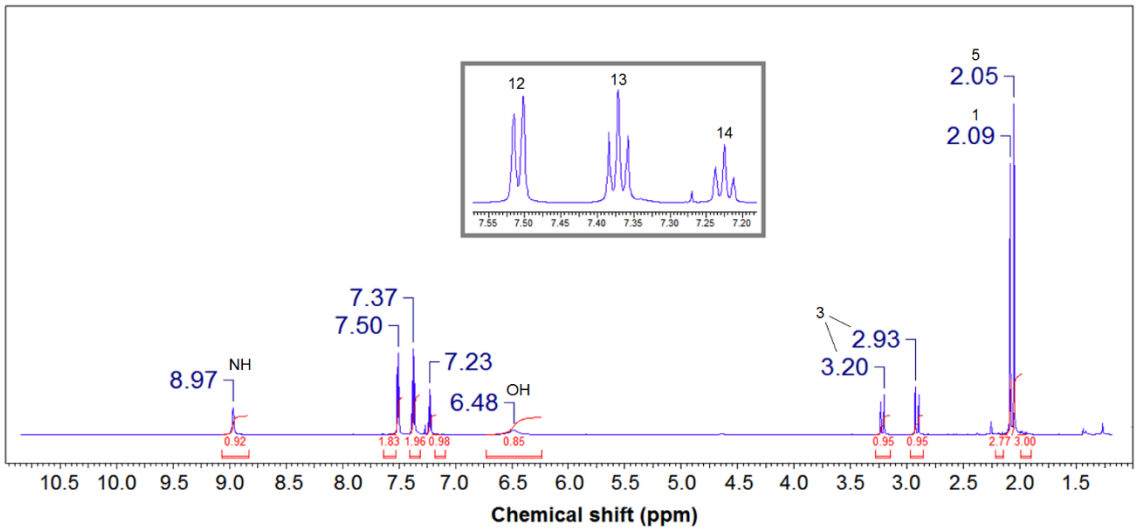

Fig. S6. ^{1}H NMR spectrum of **HL_4'**

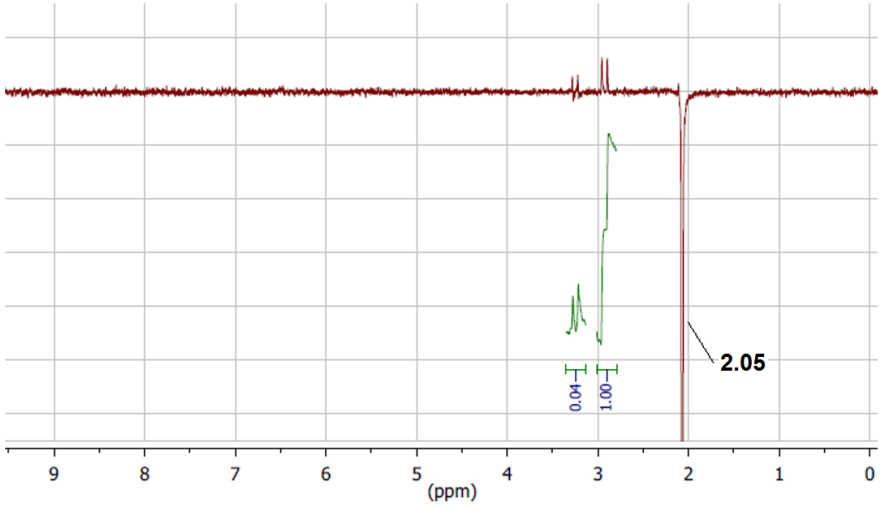

Fig. S7. 1D NOESY (2.05 ppm) NMR spectrum of **HL_4'**

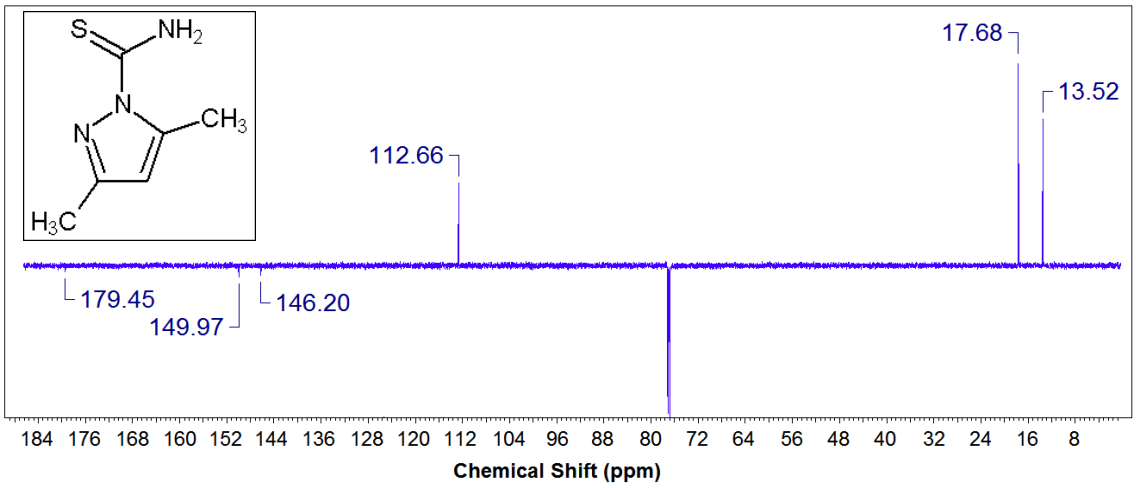

Fig. S8. DEPTQ NMR spectrum of HL_1

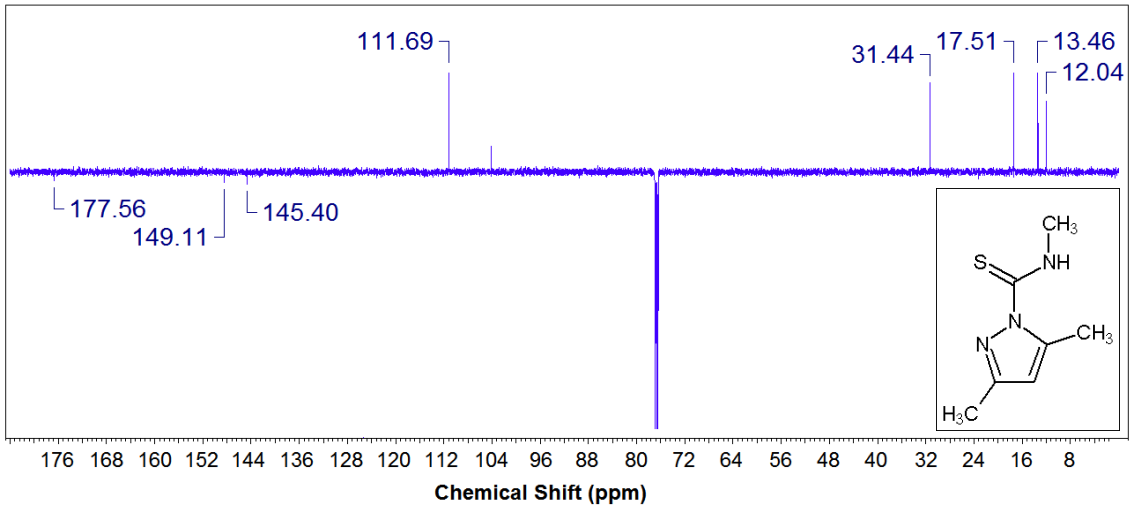

Fig. S9. DEPTQ NMR spectrum of HL_2

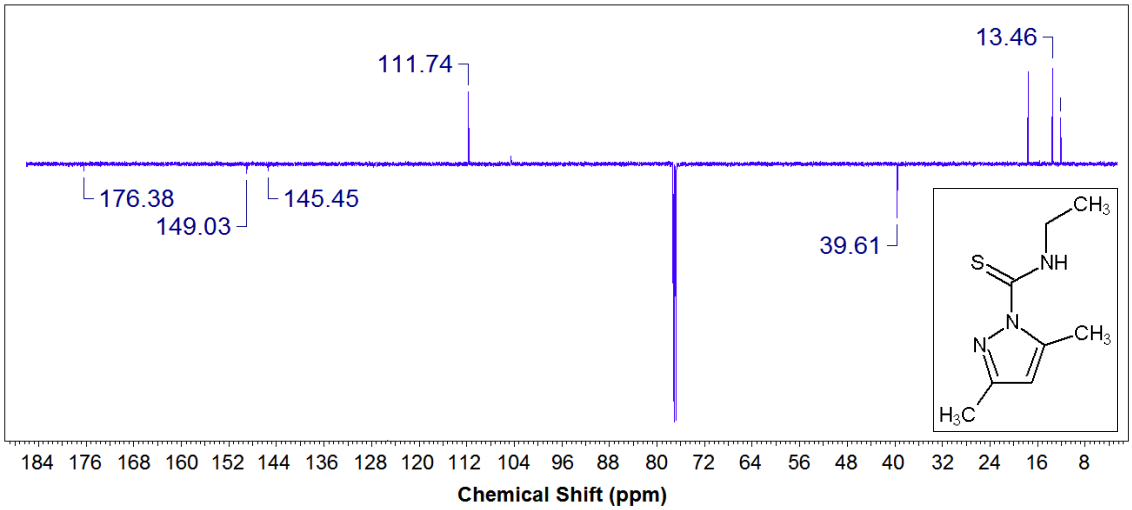

Fig. S10. DEPTQ NMR spectrum of HL_3

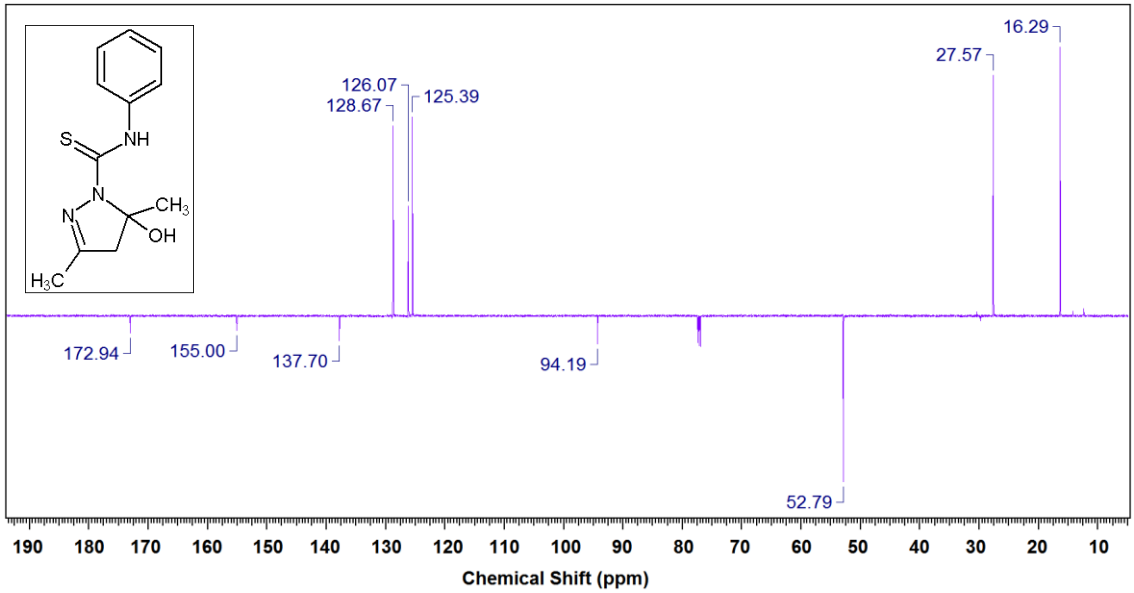

Fig. S11. DEPTQ NMR spectrum of **HL_4'**

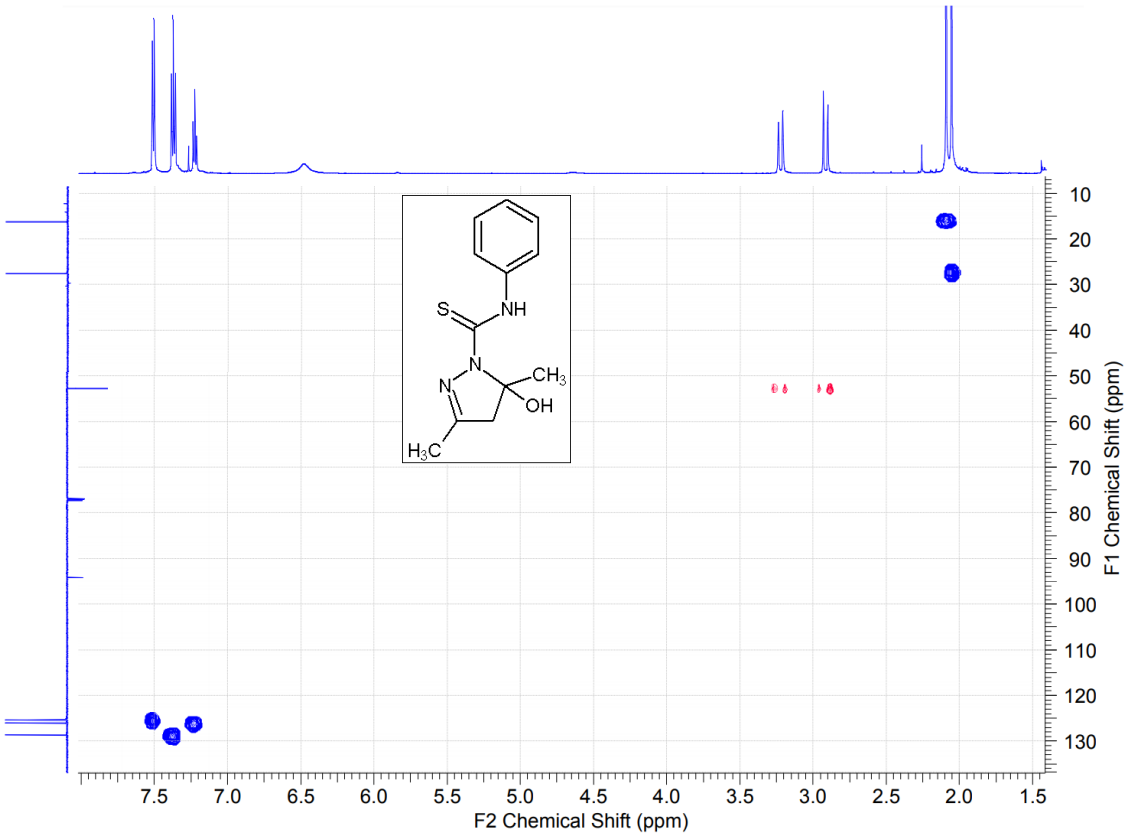

Fig. S12. ^{1}H-^{13}C HSQC NMR spectrum of **HL_4'**

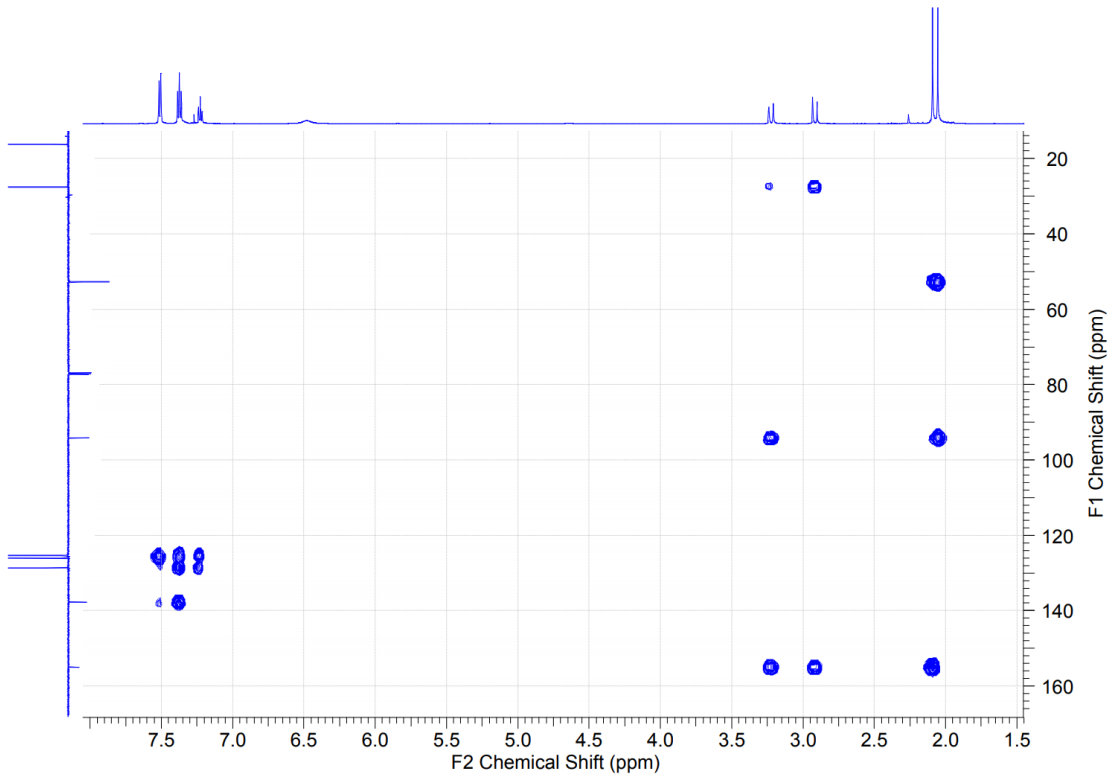

Fig. S13. ^{1}H-^{13}C HMBC NMR spectrum of **HL_4'**

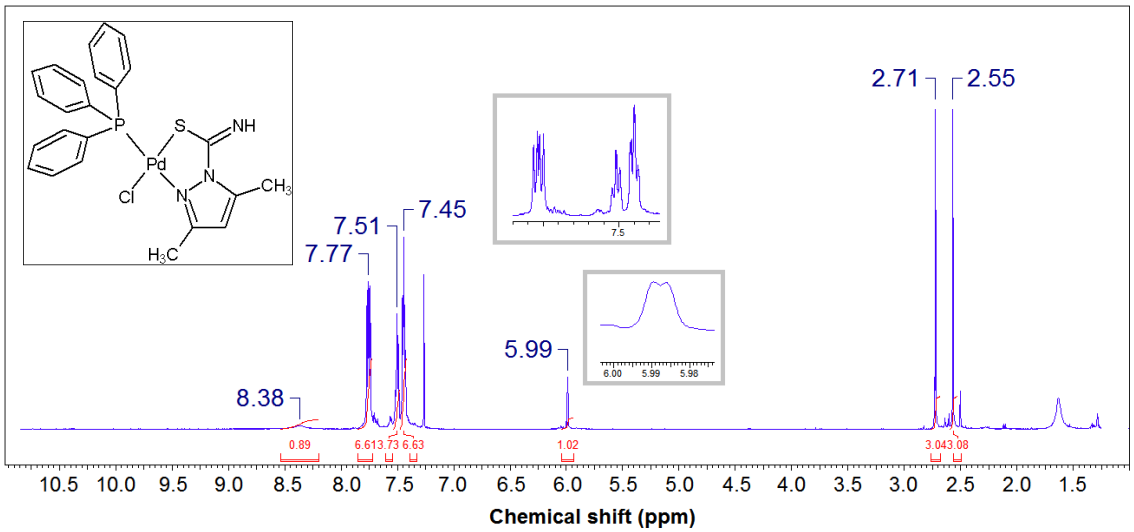

Fig. S14. ^{1}H NMR spectrum of complex **1**

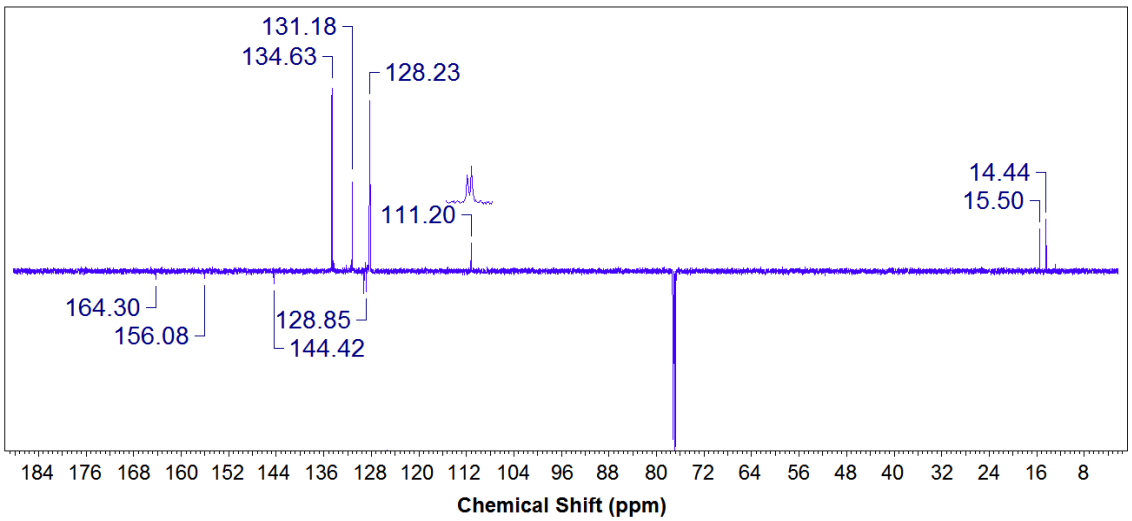

Fig. S15. DEPTQ NMR spectrum of complex **1**

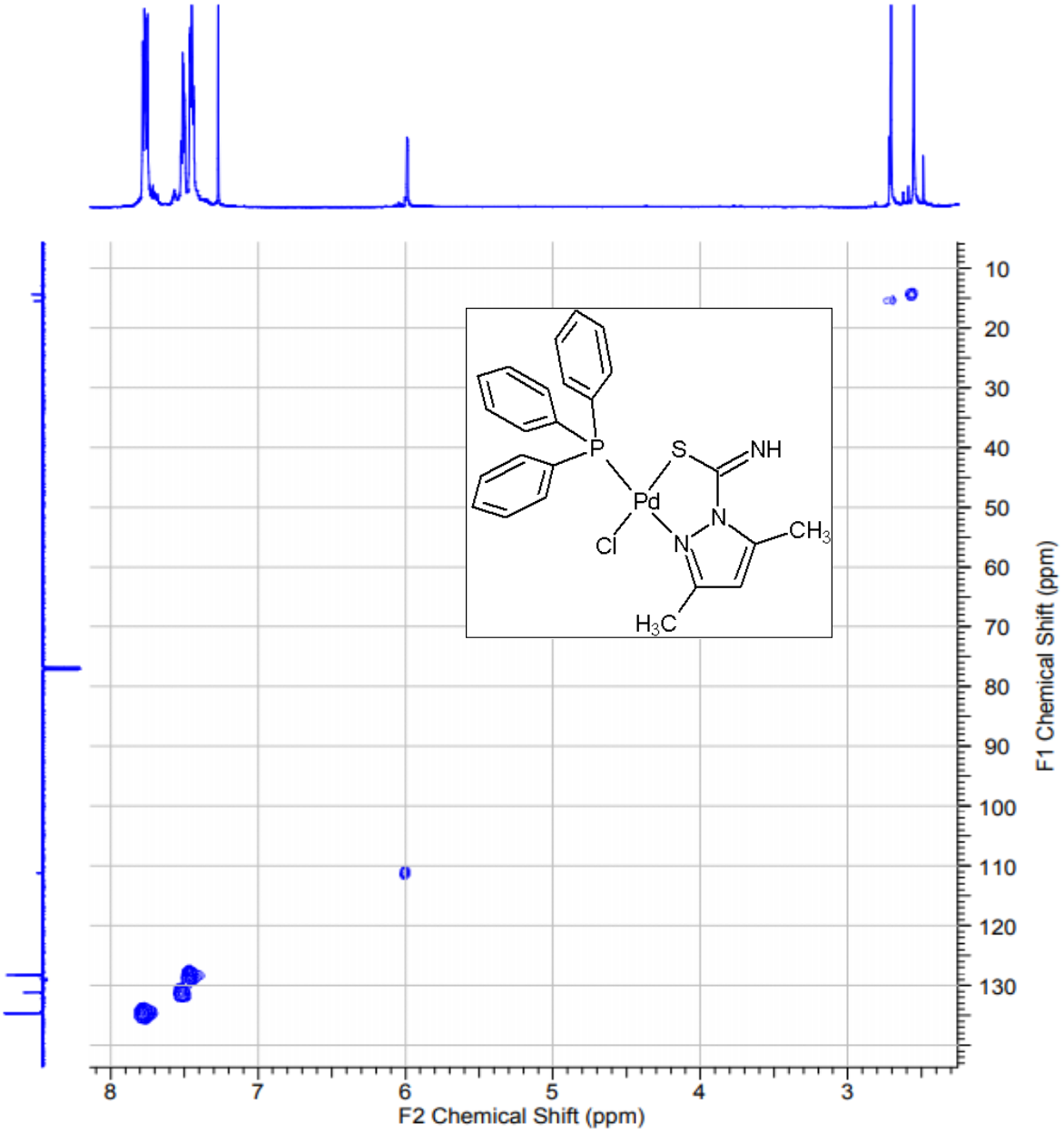

Fig. S16. ^{1}H-^{13}C HSQC NMR spectrum of complex **1**

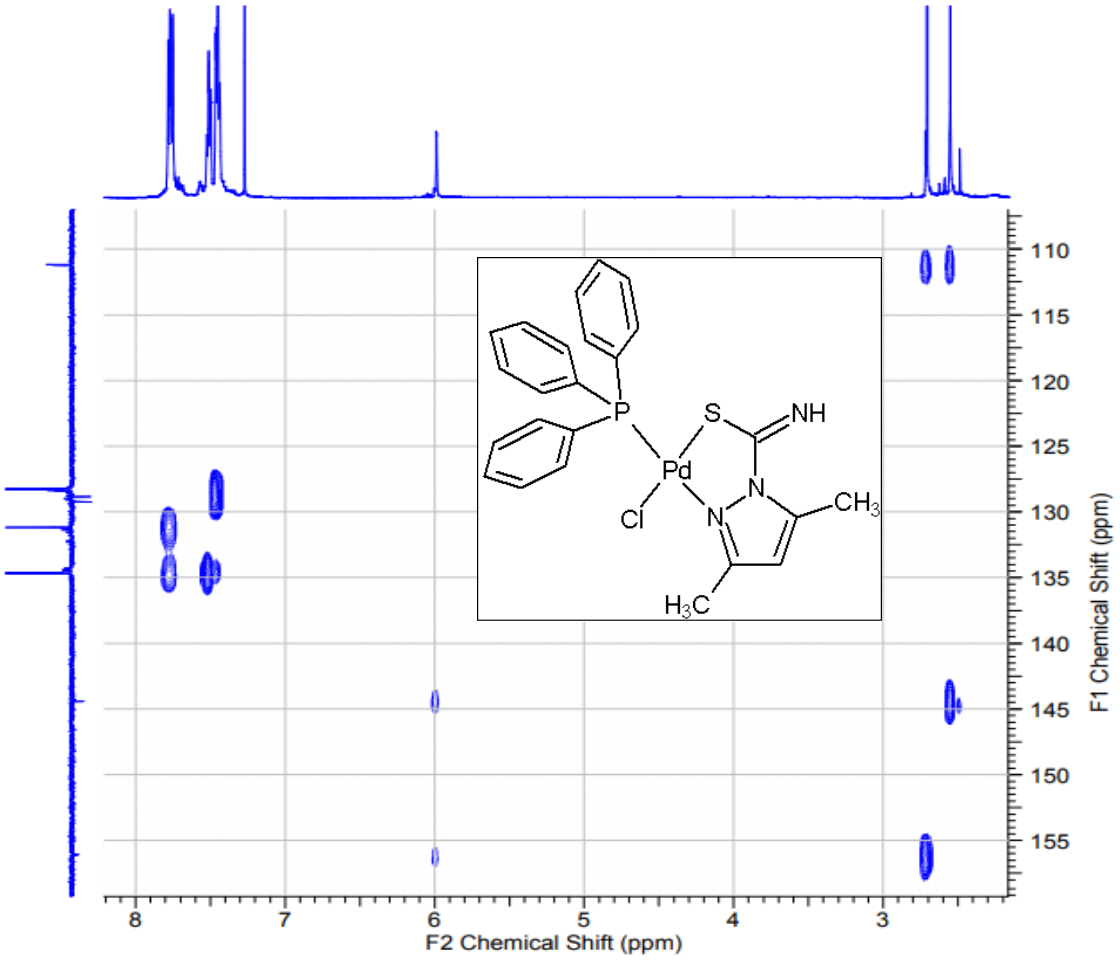

Fig. S17. ^{1}H-^{13}C HMBC NMR spectrum of complex **1**

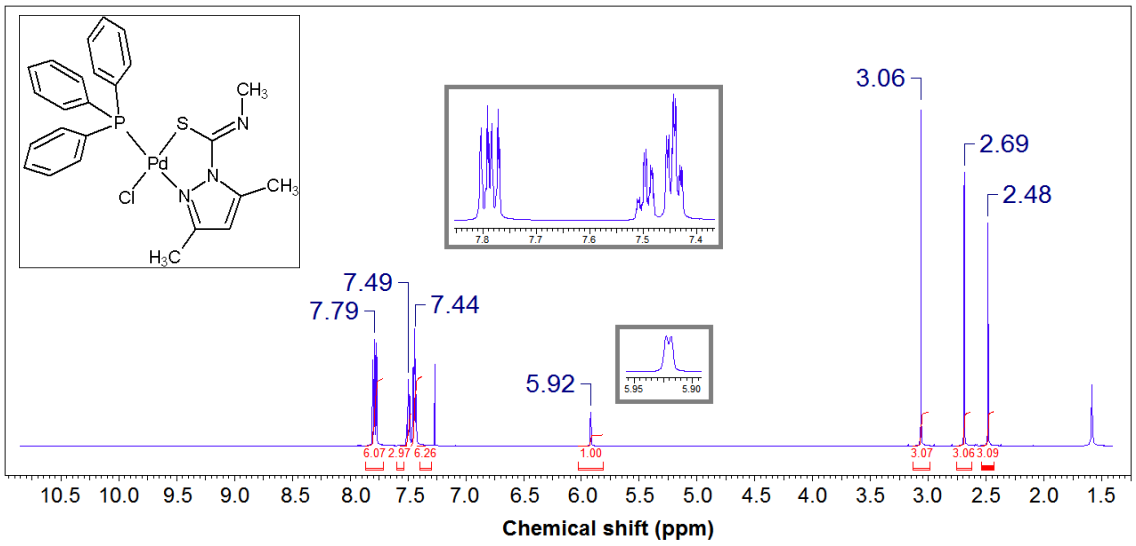

Fig. S18. ^{1}H NMR spectrum of complex **2**

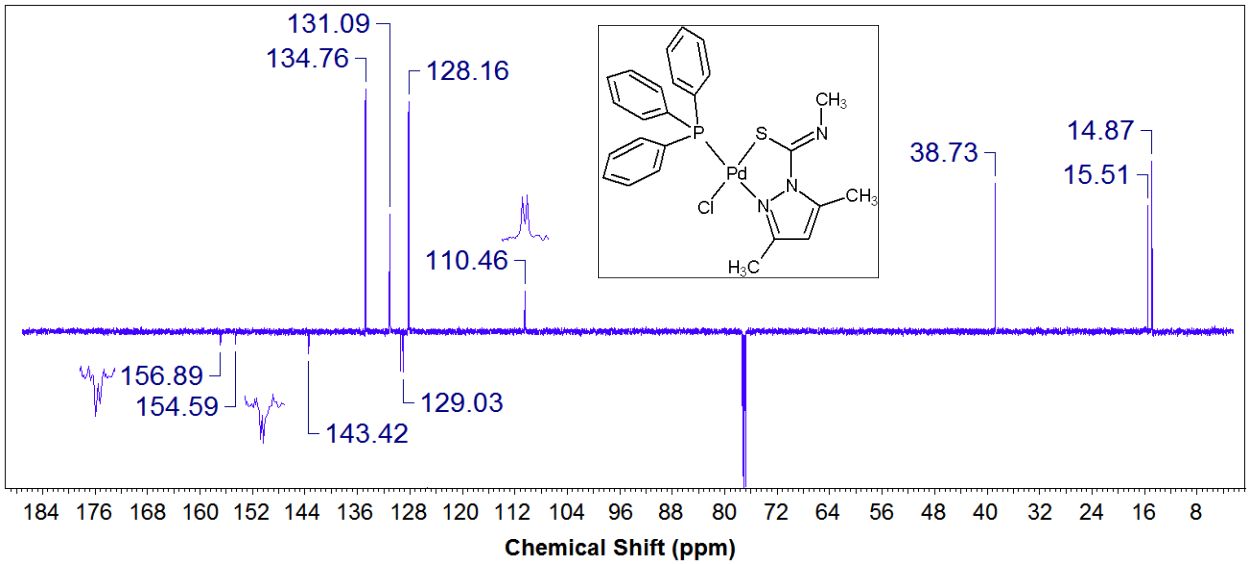

Fig. S19. DEPTQ NMR spectrum of complex **2**

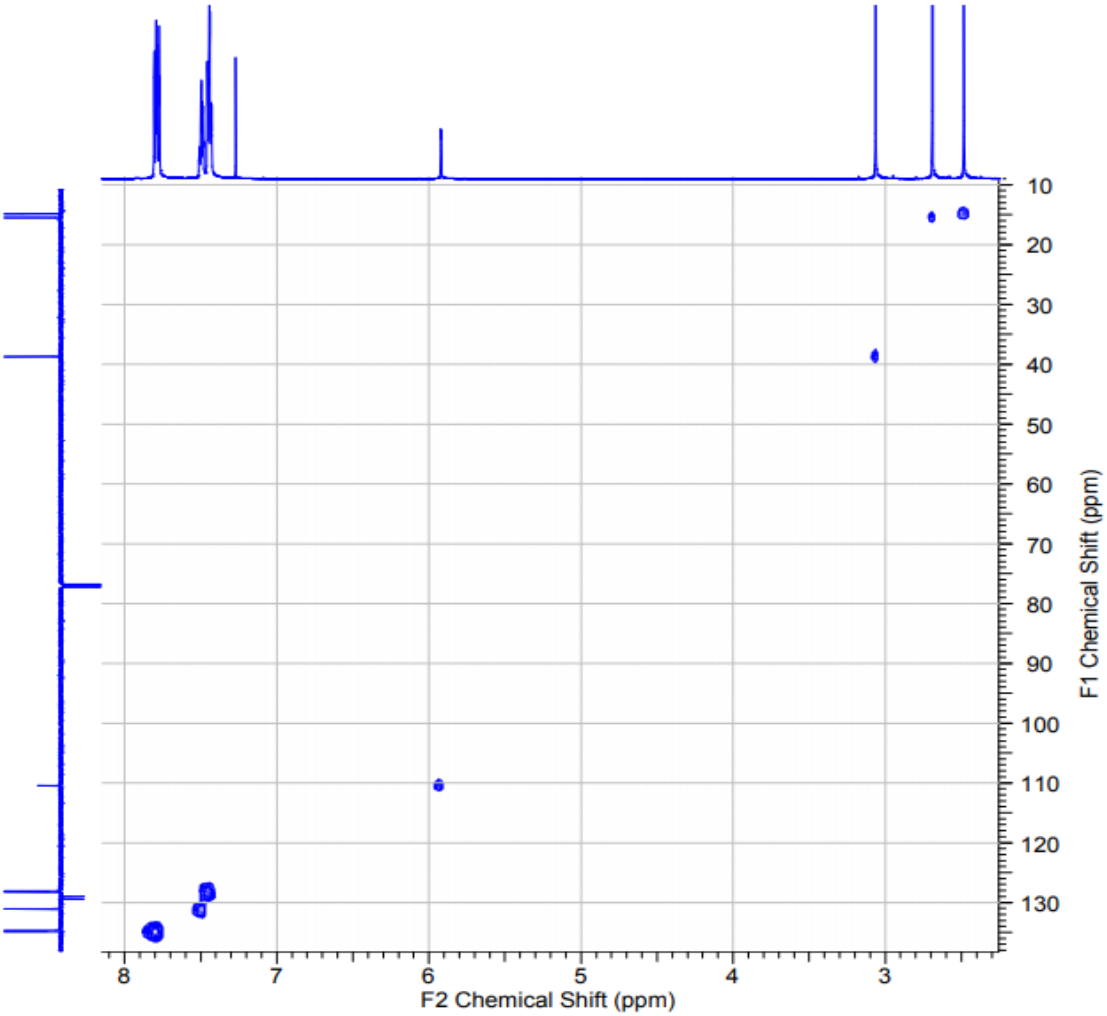

Fig. S20. ^{1}H-^{13}C HSQC NMR spectrum of complex **2**

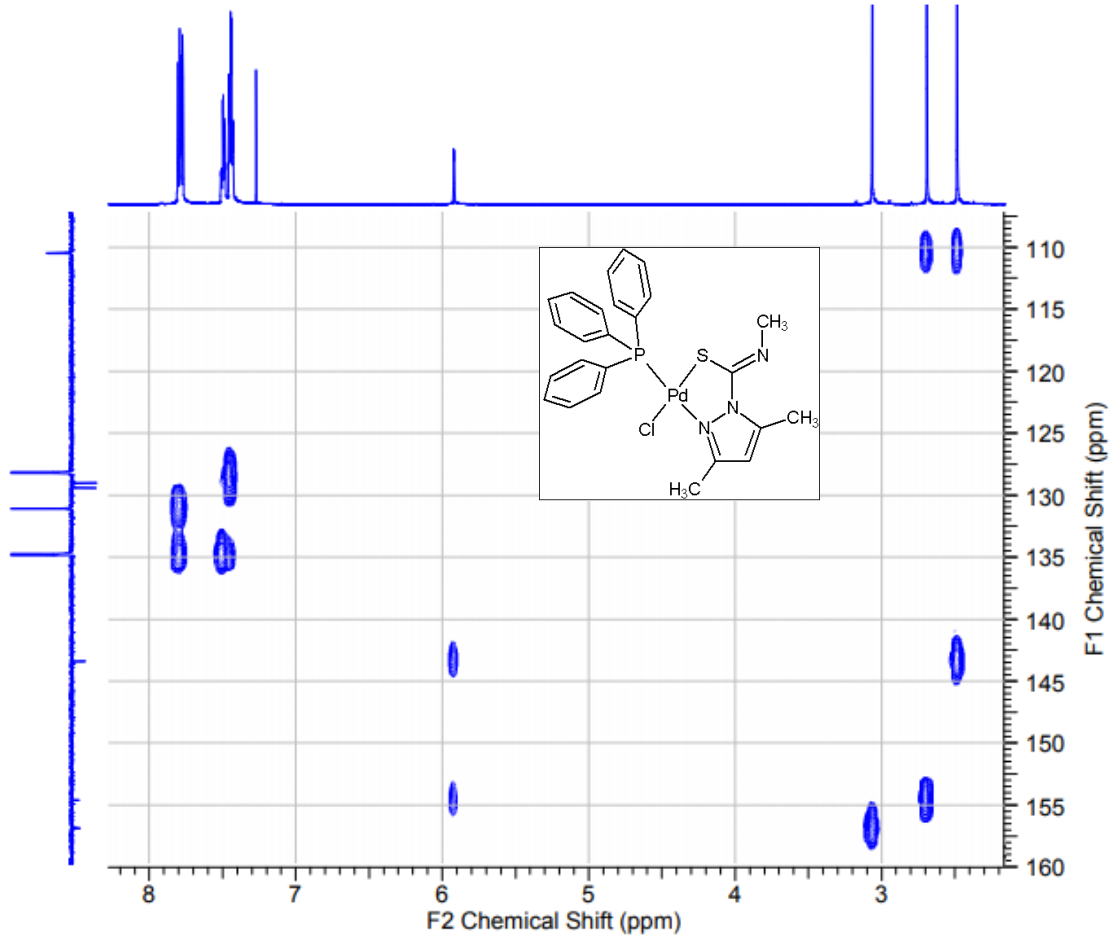

Fig. S21. ^{1}H-^{13}C HMBC NMR spectrum of complex **2**

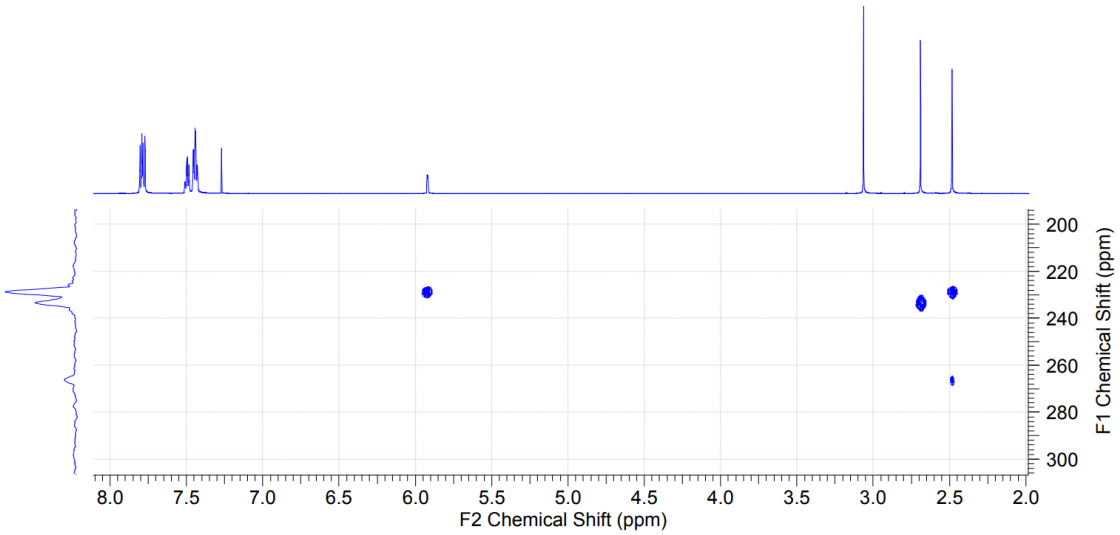

Fig. S22. ^{1}H-^{15}N HMBC NMR spectrum of complex **2**

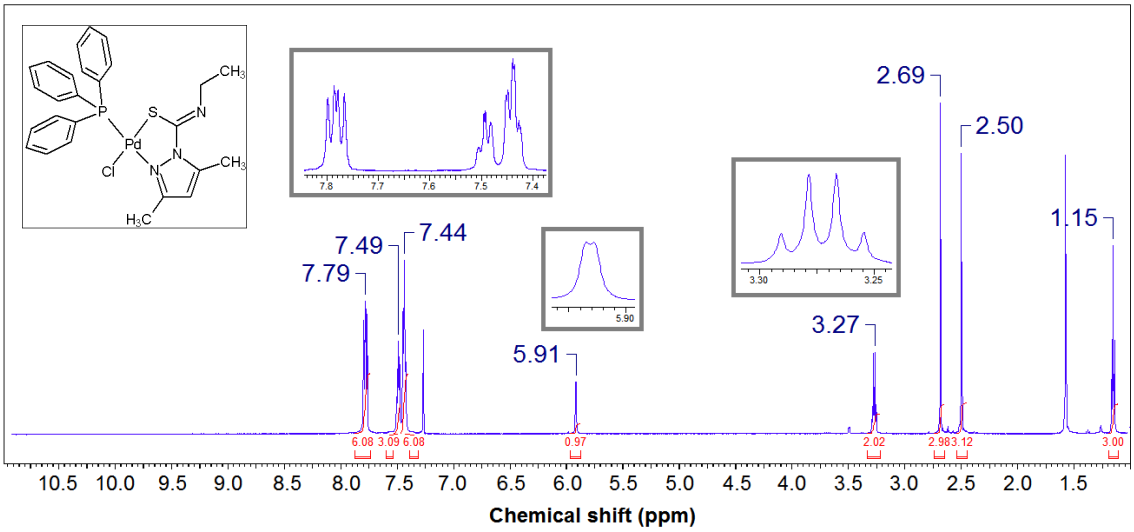

Fig. S23. ^{1}H NMR spectrum of complex **3**

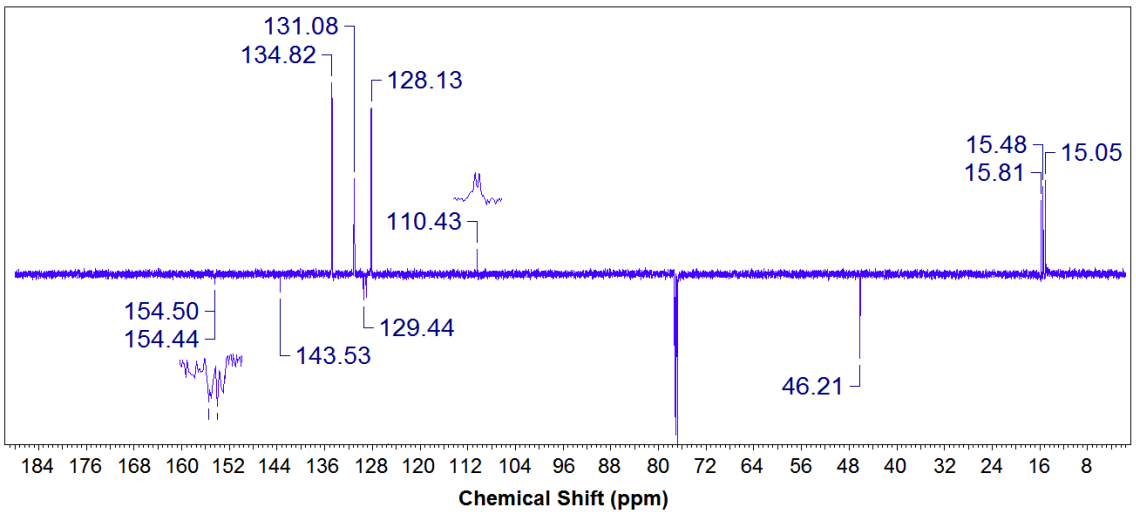

Fig. S24. DEPTQ NMR spectrum of complex **3**

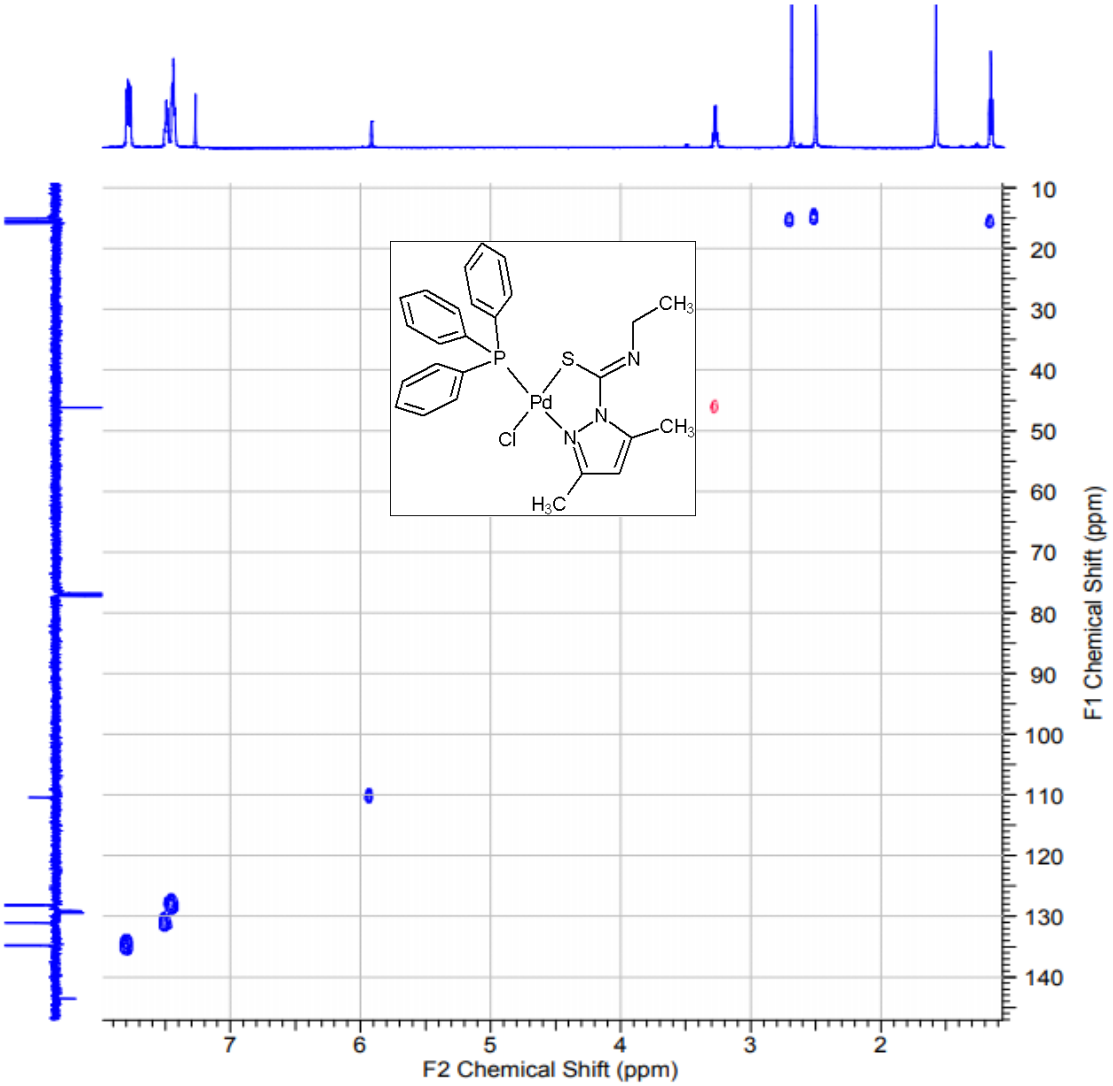

Fig. S25. ^{1}H-^{13}C HSQC NMR spectrum of complex **3**

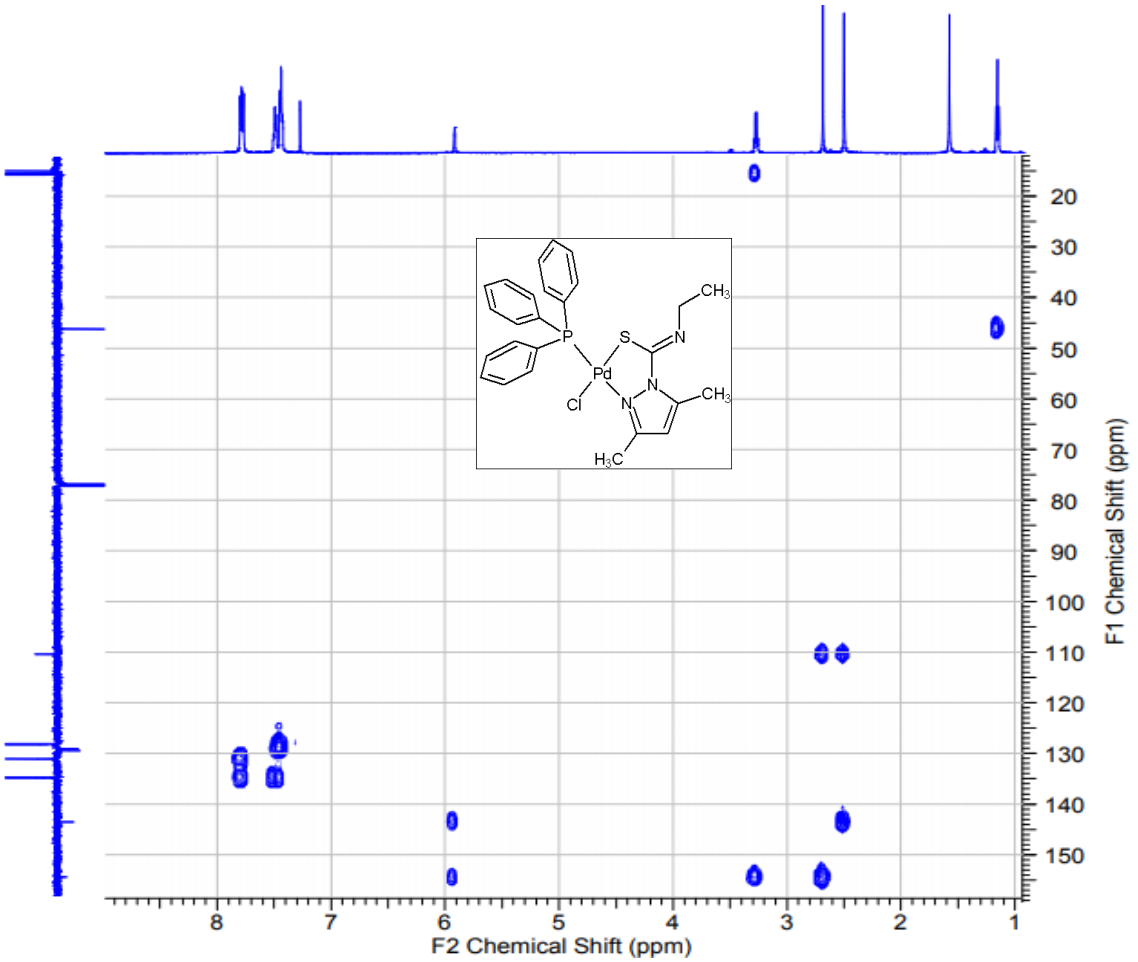

Fig. S26. ^{1}H-^{13}C HMBC NMR spectrum of complex **3**

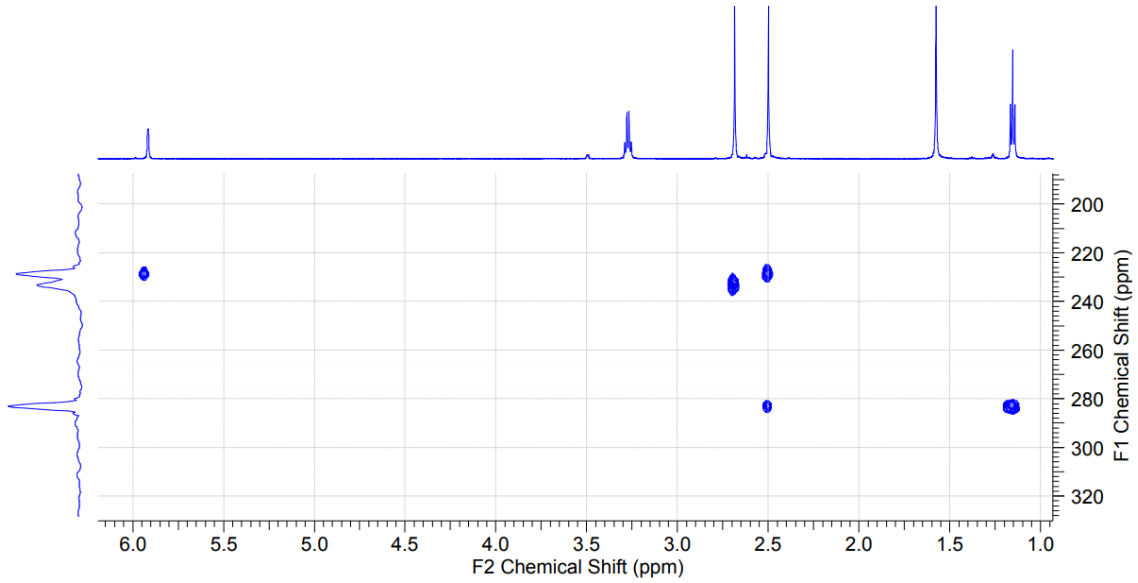

Fig. S27. ^{1}H-^{15}N HMBC NMR spectrum of complex **3**

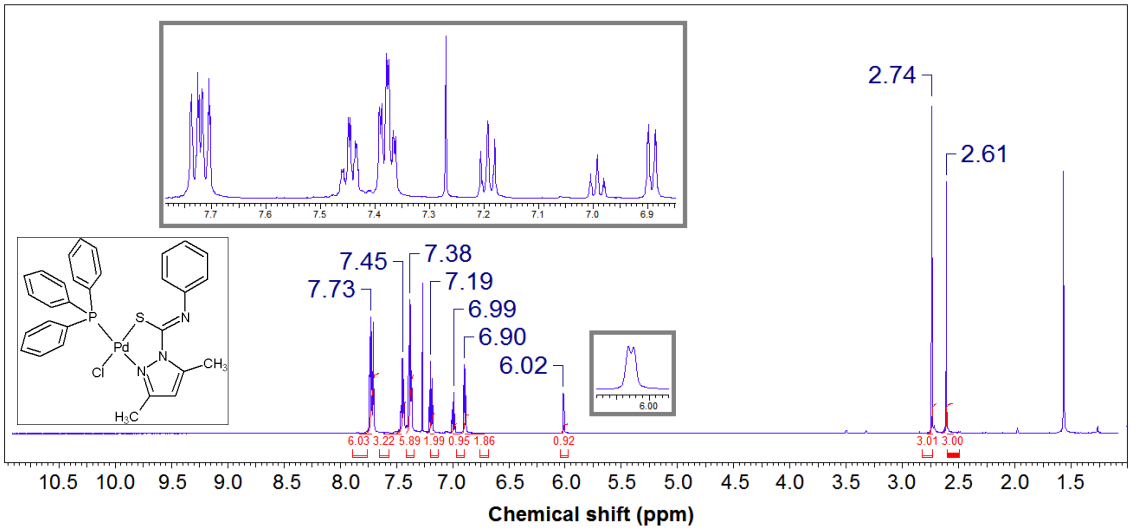

Fig. S28. ^{1}H NMR spectrum of complex **4**

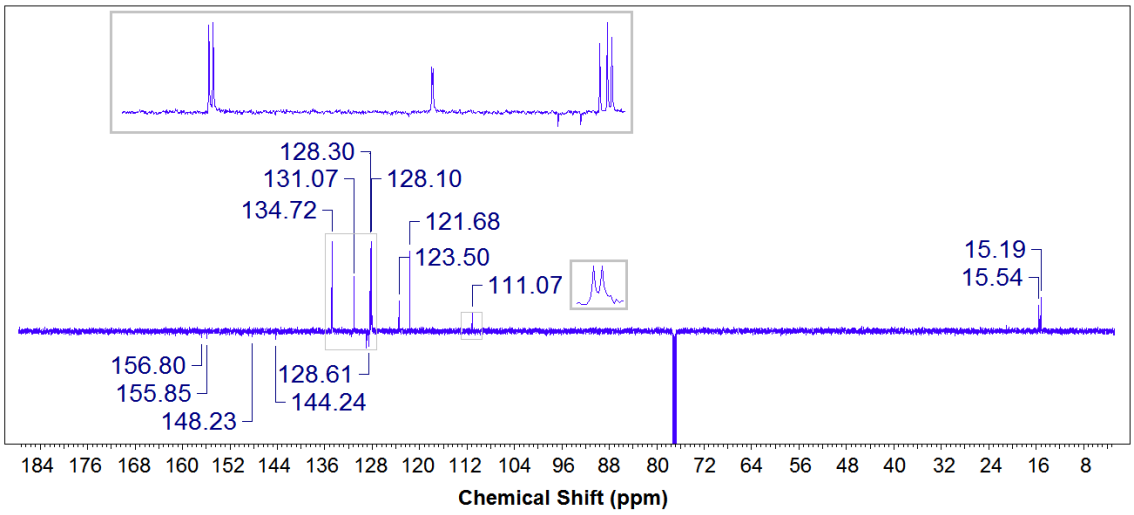

Fig. S29. DEPTQ NMR spectrum of complex **4**

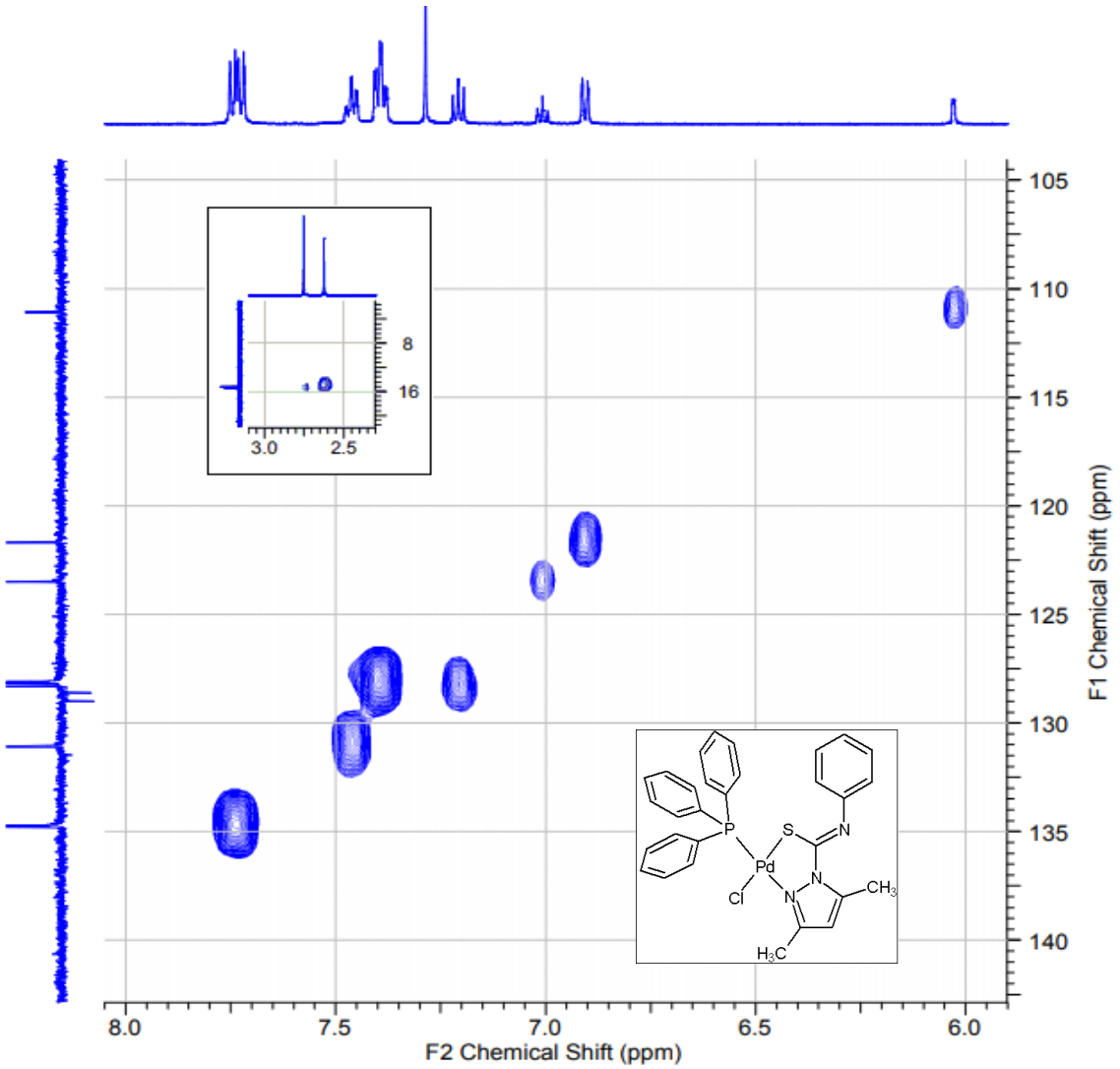

Fig. S30. ^{1}H-^{13}C HSQC NMR spectrum of complex **4**

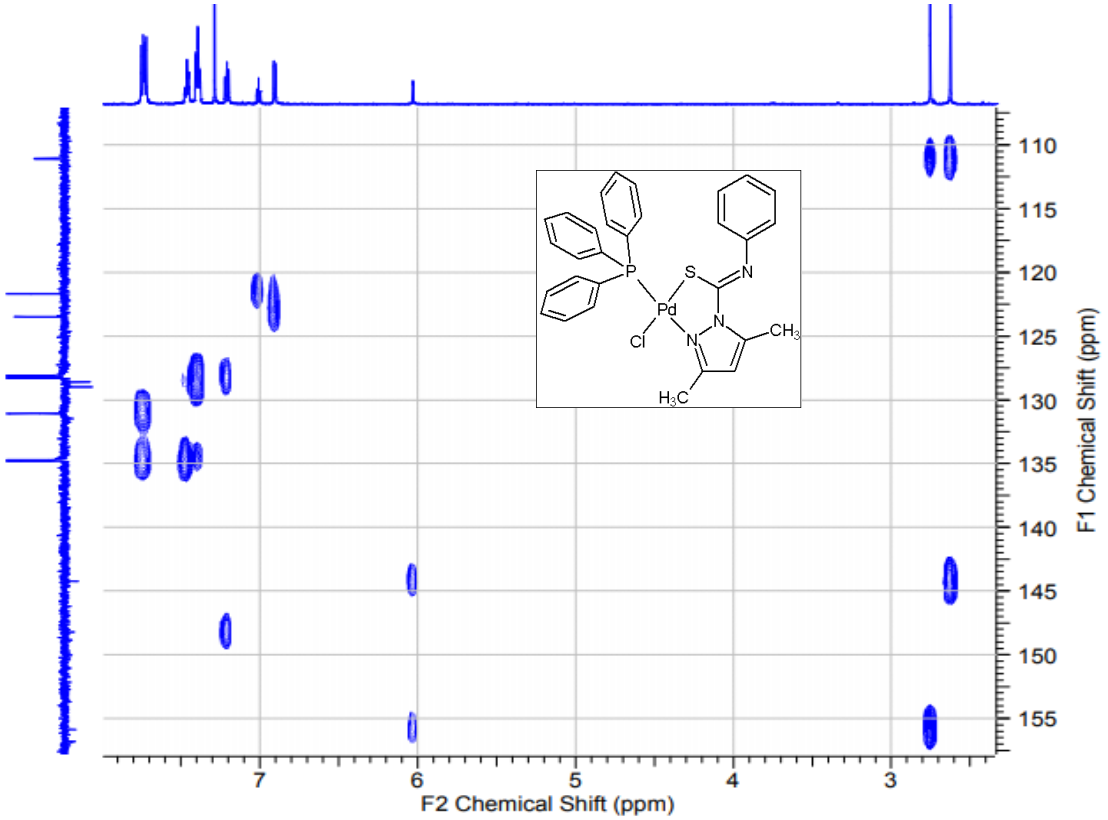

Fig. S31. ^{1}H-^{13}C HMBC NMR spectrum of complex **4**

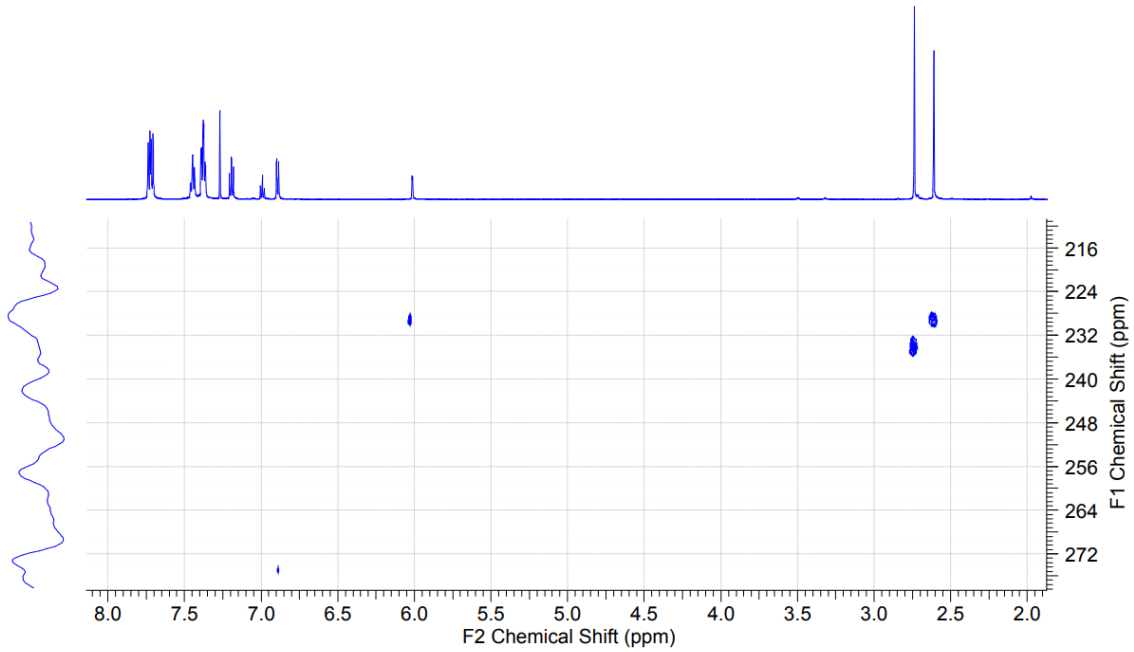

Fig. S32. ^{1}H-^{15}N HMBC NMR spectrum of complex **4**

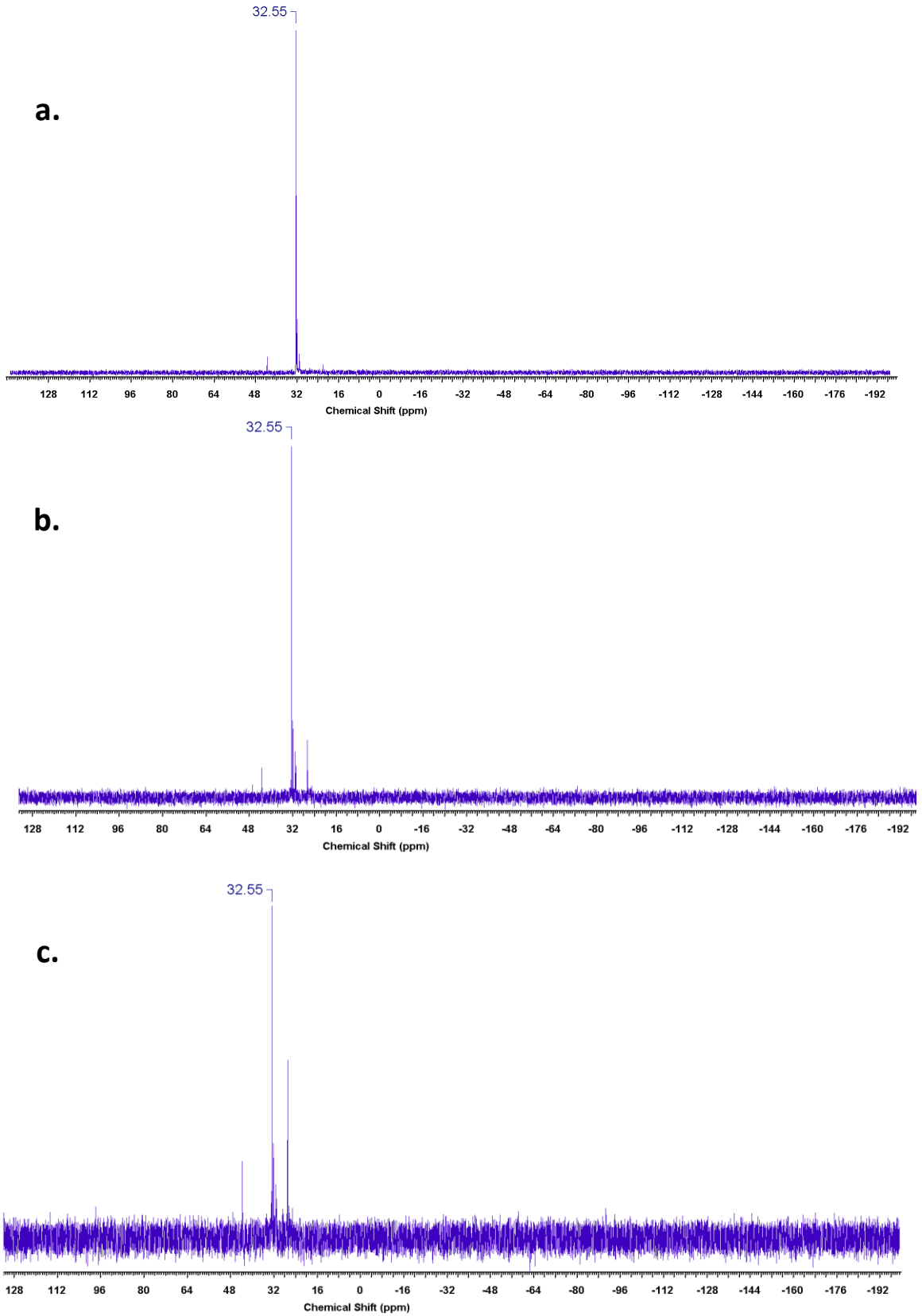

Fig. S33. ^{31}P NMR – Complex **1** in DMSO-d_6, 37°C, after 10 min (**a**), 24 h (**b**) and 48 h (**c**)

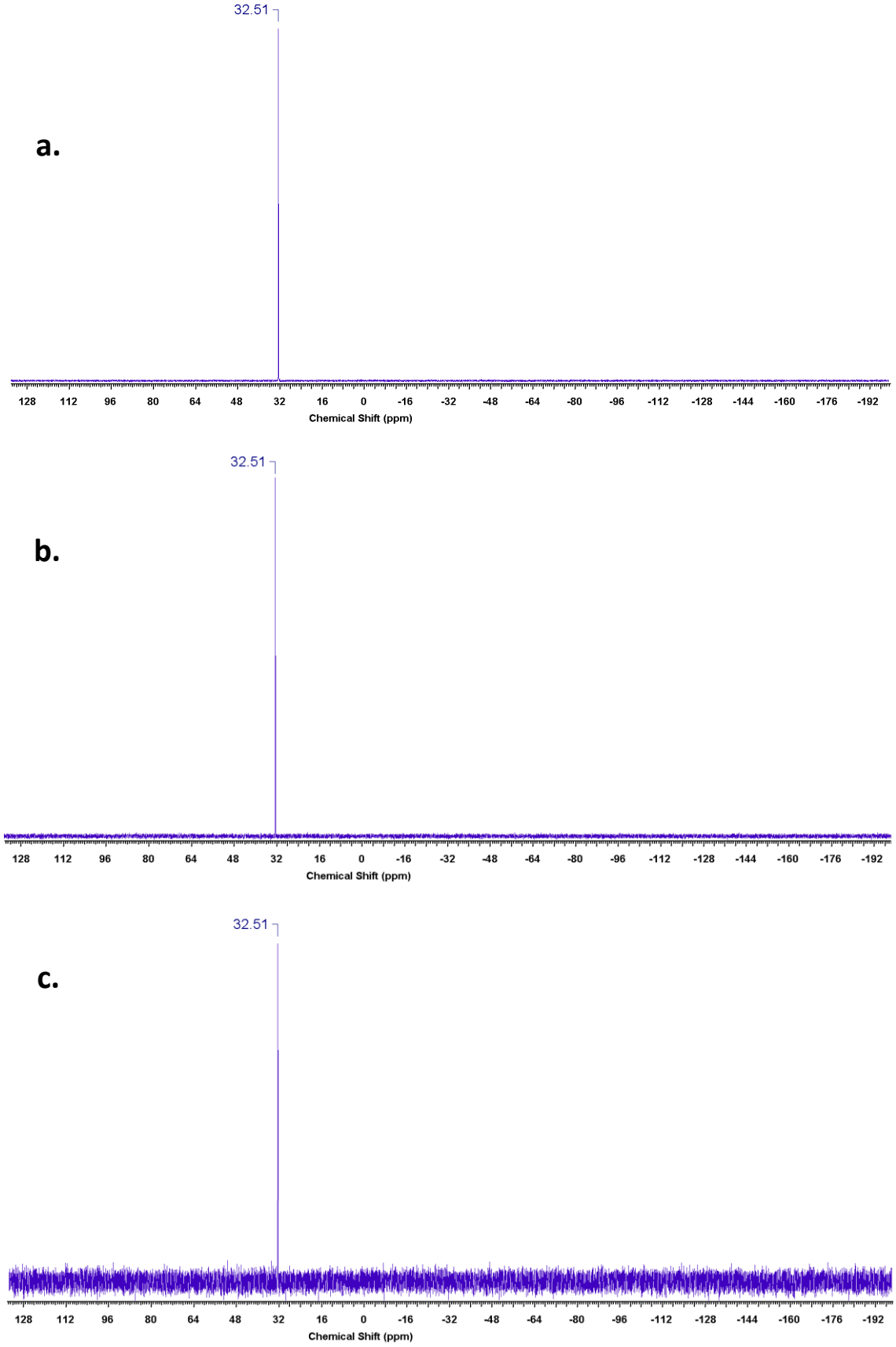

Fig. S34. ^{31}P NMR – Complex **2** in DMSO-d_6, 37°C, after 10 min (**a**), 24 h (**b**) and 48 h (**c**)

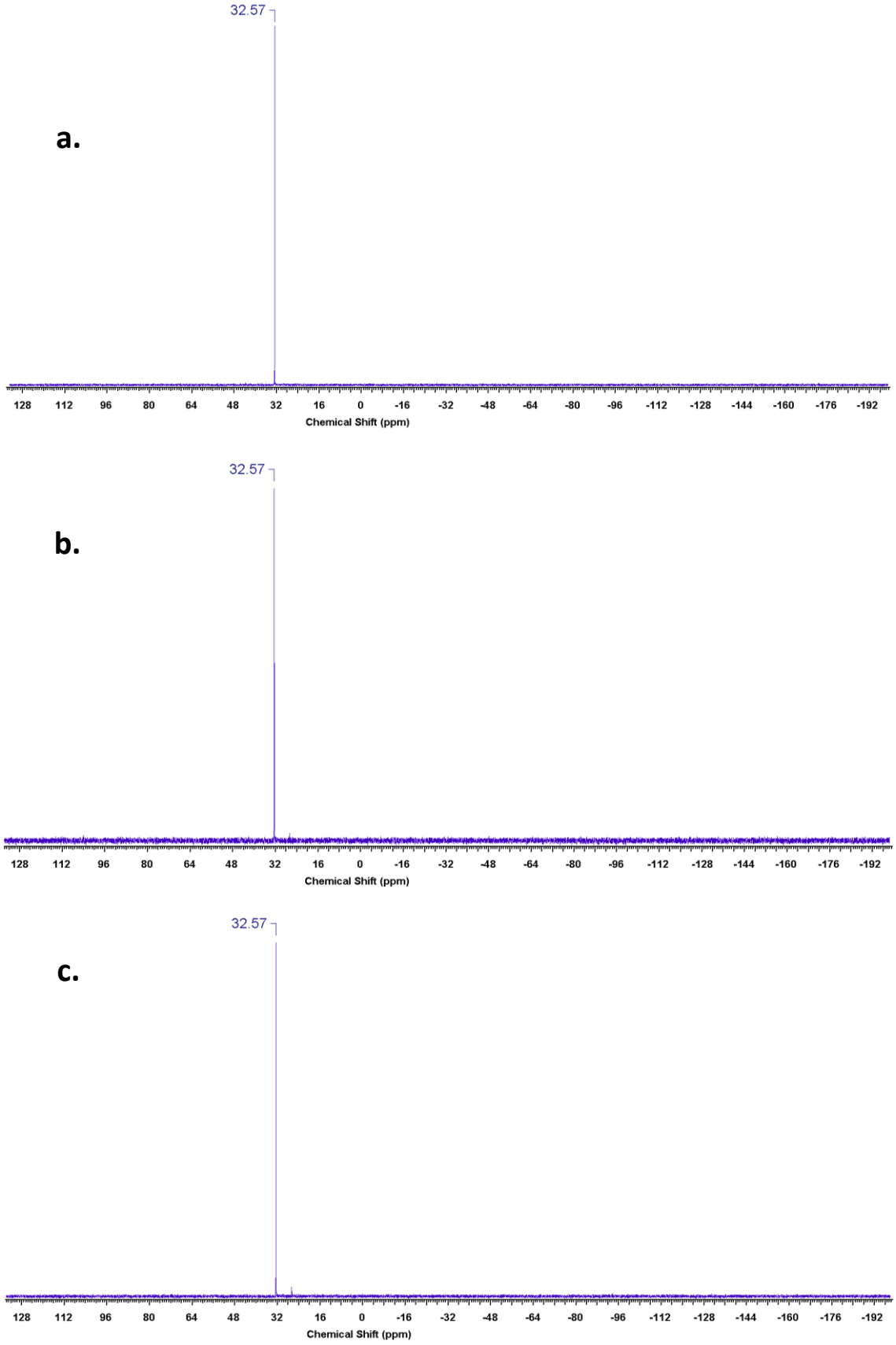

Fig. S35. ^{31}P NMR – Complex **3** in DMSO-d_6, 37°C, after 10 min (**a**), 24 h (**b**) and 48 h (**c**)

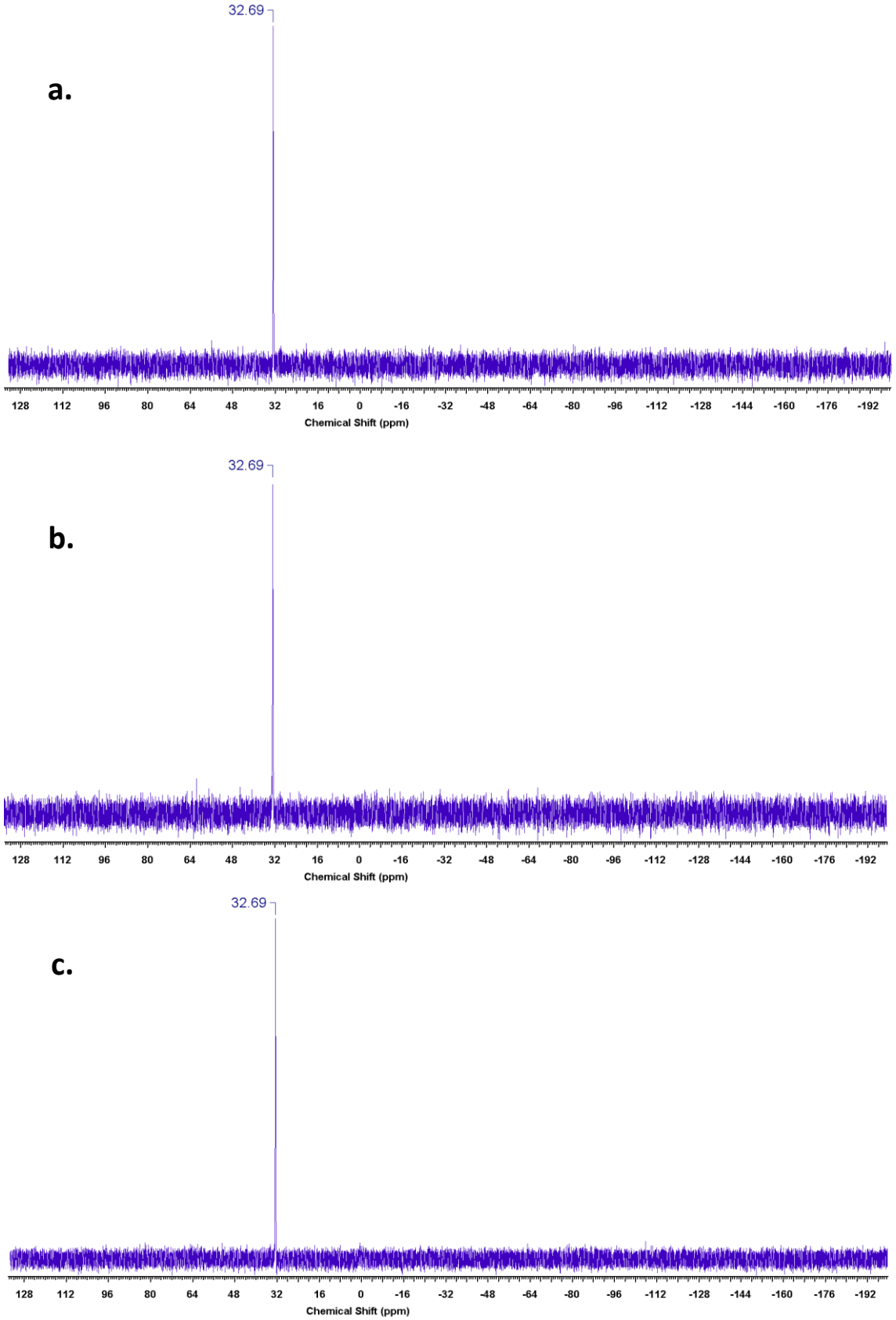

Fig. S36. ^{31}P NMR – Complex **4** in DMSO-d_6, 37°C, after 10 min (**a**), 24 h (**b**) and 48 h (**c**)

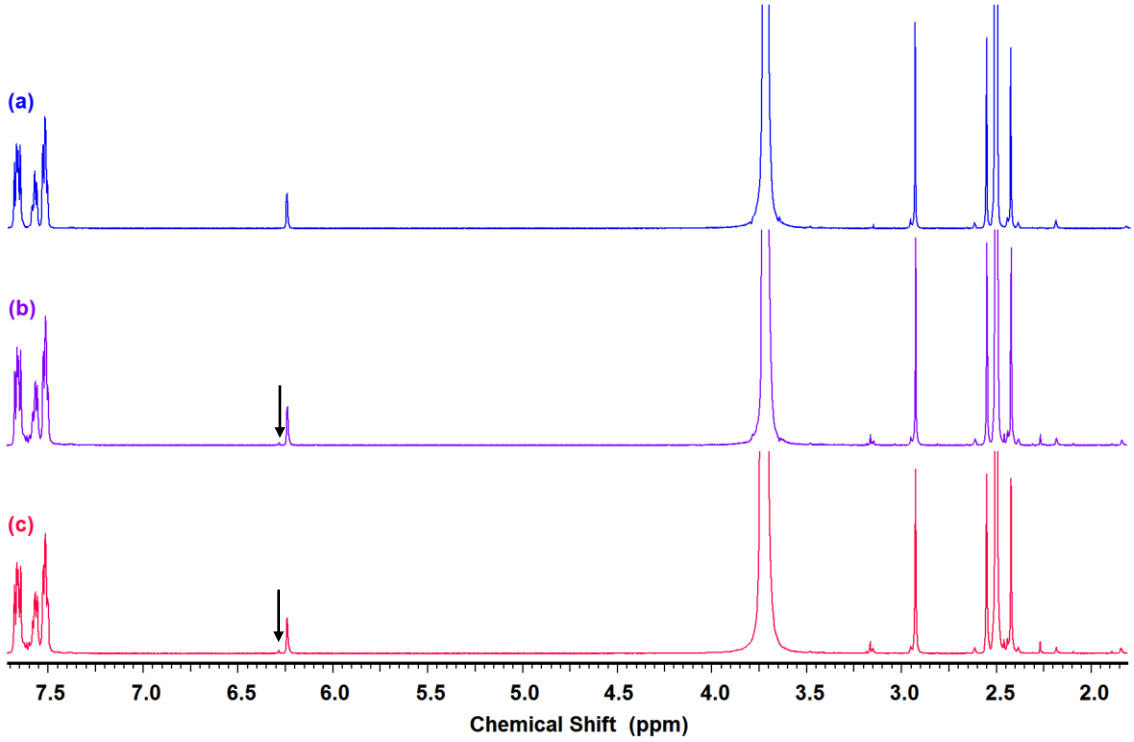

Fig. S37. ^{1}H NMR – Complex **2** after 7 minutes (**a**), 24 (**b**) and 48 (**c**) hours in solution of DMSO-d_6/D_2O (70%/30%) in PBS (10 μM; pH = 7.3)

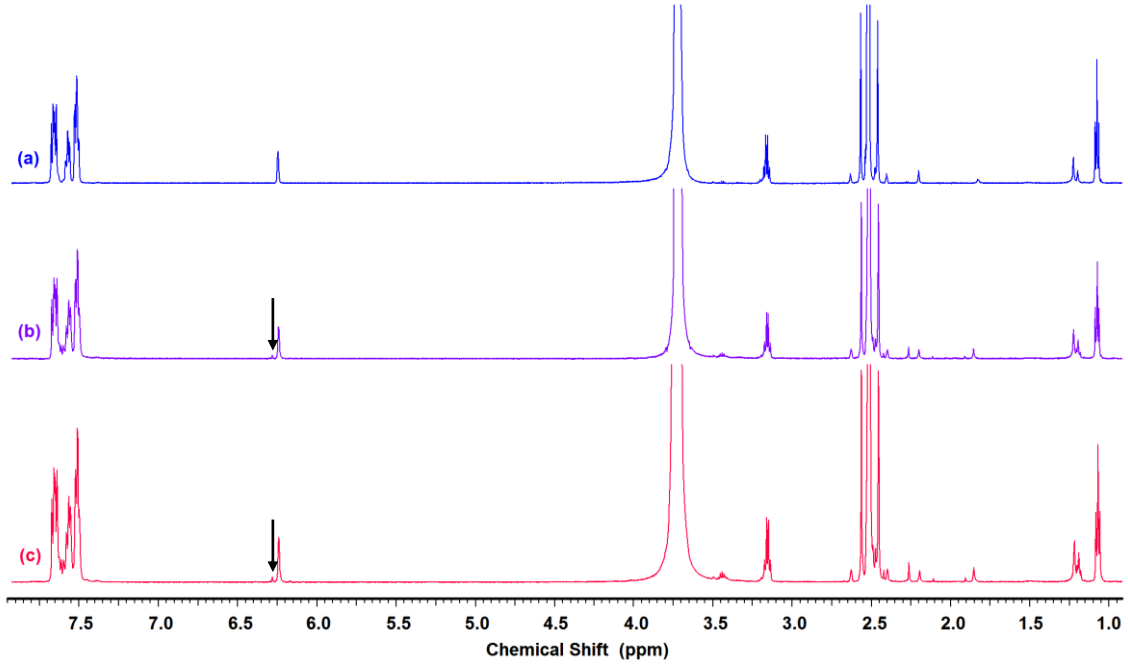

Fig. S38. ^{1}H NMR – Complex **3** after 12 minutes (**a**), 24 (**b**) and 48 (**c**) hours in solution of DMSO-d_6/D_2O (70%/30%) in PBS (pH = 7.3)

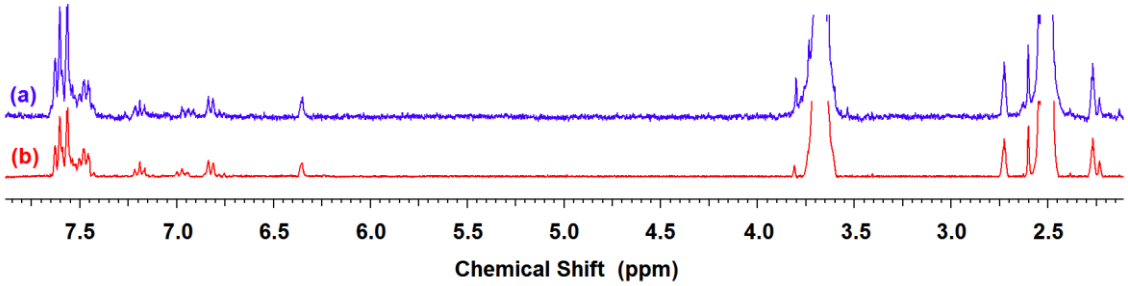

Fig. S39. ^{1}H NMR – Complex **4** after 18 minutes (**a**), and 48 (**b**) hours in solution of DMSO-d_6/D_2O (70%/30%) in PBS (pH = 7.3)

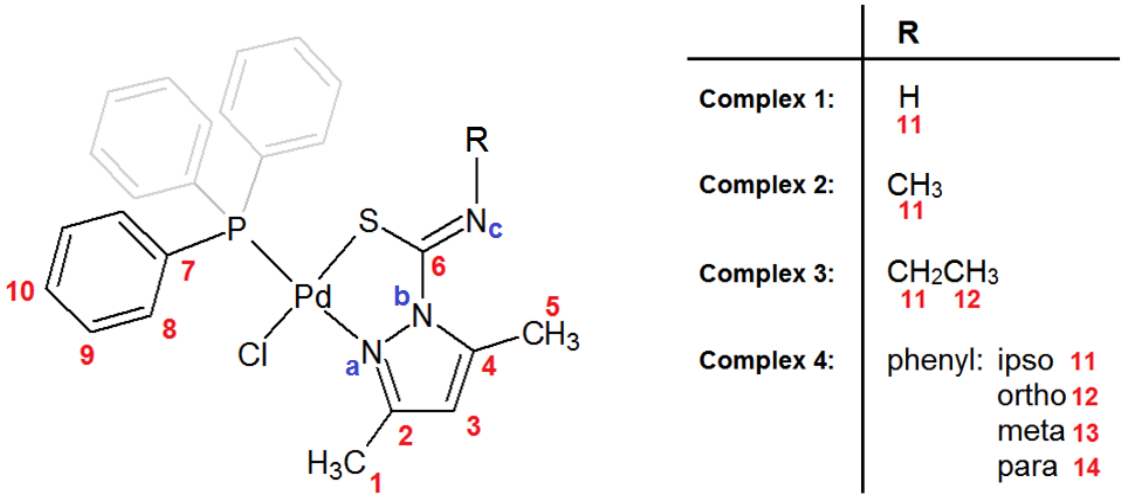

Fig. S40. Numbering for ligands and complexes for NMR assignments

Table S2. ^{1}H (600MHz) and ^{13}C-DEPTQ (150 MHz) NMR Spectroscopic Data Assignments (in DMSO-d_6) for compounds **1**-**4**. (δ in ppm, J in Hz)

Compound	Complex 1		Complex 2		Complex 3		Complex 4	
Position	^{1}H	^{13}C	^{1}H	^{13}C	^{1}H	^{13}C	^{1}H	^{13}C
1	2.71 (s)	15.5	2.69 (s)	15.5	2.69 (s)	15.5	2.74 (s)	15.5
2	-	156.1 (d) $^{3}J_{CP}$ = 3.3	-	154.6 (d) $^{3}J_{CP}$ = 3.3	-	154.5 (d) $^{3}J_{CP}$ = 2.2	-	155.8 $^{3}J_{CP}$ = 3.3
3	5.99 (d) $^{5}J_{HP}$ = 2.0	111.2 (d) $^{4}J_{CP}$ = 5.5	5.92 (d) $^{5}J_{HP}$ = 2.6	110.5 (d) $^{4}J_{CP}$ = 5.5	5.91 (d) $^{5}J_{HP}$ = 1.8	110.4 (d) $^{4}J_{CP}$ = 4.4	6.02 (d) $^{5}J_{HP}$ = 2.2	111.1 (d) $^{4}J_{CP}$ = 5.5
4	-	144.4	-	143.4	-	143.5	-	144.2
5	2.55 (s)	14.4	2.48 (s)	14.9	2.50 (s)	15.05	2.61 (s)	15.2
6	-	164.3 (d) $^{3}J_{CP}$ = 5.5	-	156.9 (d) $^{3}J_{CP}$ = 5.5	-	154.4 (d) $^{3}J_{CP}$ = 5.5	-	156.8 (d) $^{3}J_{CP}$ = 4.4
7	-	128.8 (d) $^{1}J_{CP}$ = 57.5	-	129.03 (d) $^{1}J_{CP}$ = 57.5	-	129.44 (d) $^{1}J_{CP}$ = 57.5	-	128.6 (d) $^{1}J_{CP}$ = 57.5
8	7.77 (m)	134.6 (d) $^{2}J_{CP}$ = 11.1	7.79 (m)	134.8 (d) $^{2}J_{CP}$ = 11.1	7.79 (m)	134.8 (d) $^{2}J_{CP}$ = 11.1	7.73 (m)	134.7 (d) $^{2}J_{CP}$ = 11.1
9	7.45 (m)	128.2 (d) $^{3}J_{CP}$ = 12.2	7.44 (m)	128.2 (d) $^{3}J_{CP}$ = 11.1	7.44 (m)	128.1 (d) $^{3}J_{CP}$ = 12.2	7.38 (m)	128.1 (d) $^{3}J_{CP}$ = 11.1
10	7.51 (m)	131.2 (d) $^{4}J_{CP}$ = 2.2	7.49 (m)	131.1 (d) $^{4}J_{CP}$ = 3.3	7.49 (m)	131.1 (d) $^{4}J_{CP}$ = 2.2	7.45 (m)	131.1 (d) $^{4}J_{CP}$ = 3.3
11	8.38 (br)		3.06 (s)	38.7	3.27 (q) $^{3}J_{HH}$ = 7.2	46.2	-	148.2
12	-	-	-	-	1.15 (t) $^{3}J_{HH}$ = 7.2	15.8	6.90 (m)	121.7
13	-	-	-	-	-	-	7.19 (m)	128.3
14	-	-	-	-	-	-	6.99 (tt) $^{3}J_{HH}$ = 7.3	123.5

Table S3. HMBC ^{15}N and ^{31}P NMR Spectroscopic Data Assignments (in DMSO-d_6) for compounds **1**-**4**. (δ in ppm)

Compound	Complex 1	Complex 2	Complex 3	Complex 4
$^{15}N_{(a)}$	-	233.4	233.2	234.1
$^{15}N_{(b)}$	-	228.6	228.6	229.1
$^{15}N_{(c)}$	-	266.2	283.1	274.9
^{31}P	32.55	32.51	32.57	32.69

S2.2. Infrared Spectroscopy

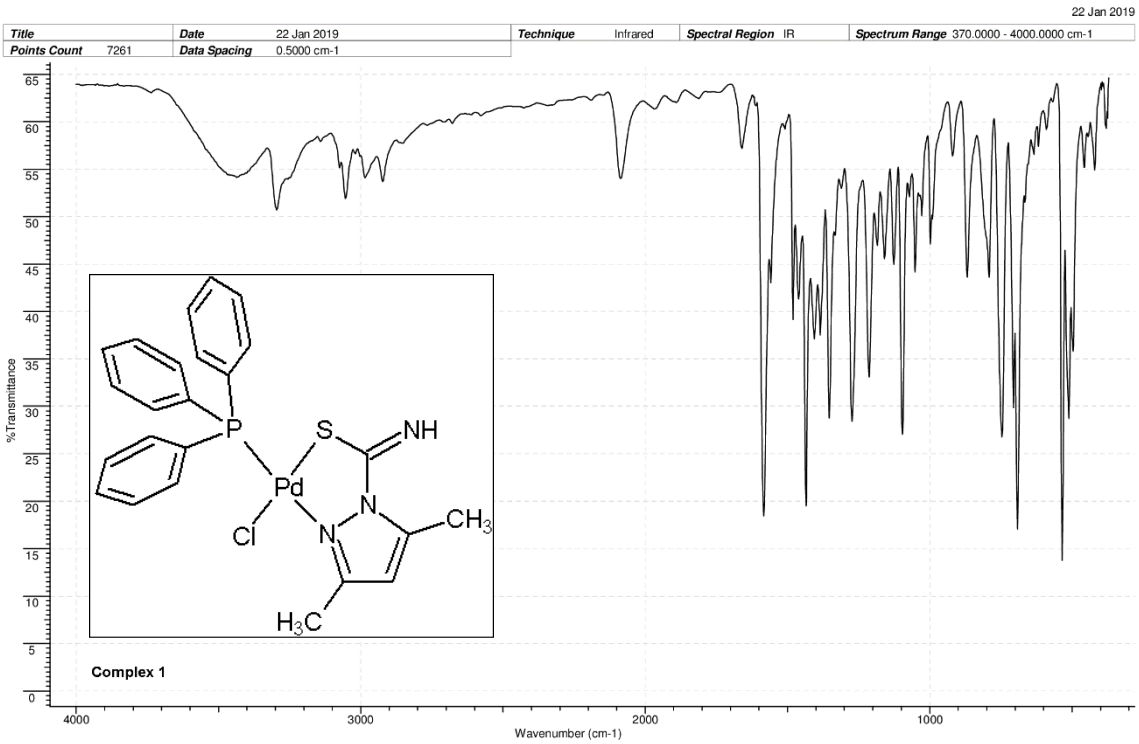

Fig. S41. Infrared spectra of complex **1**

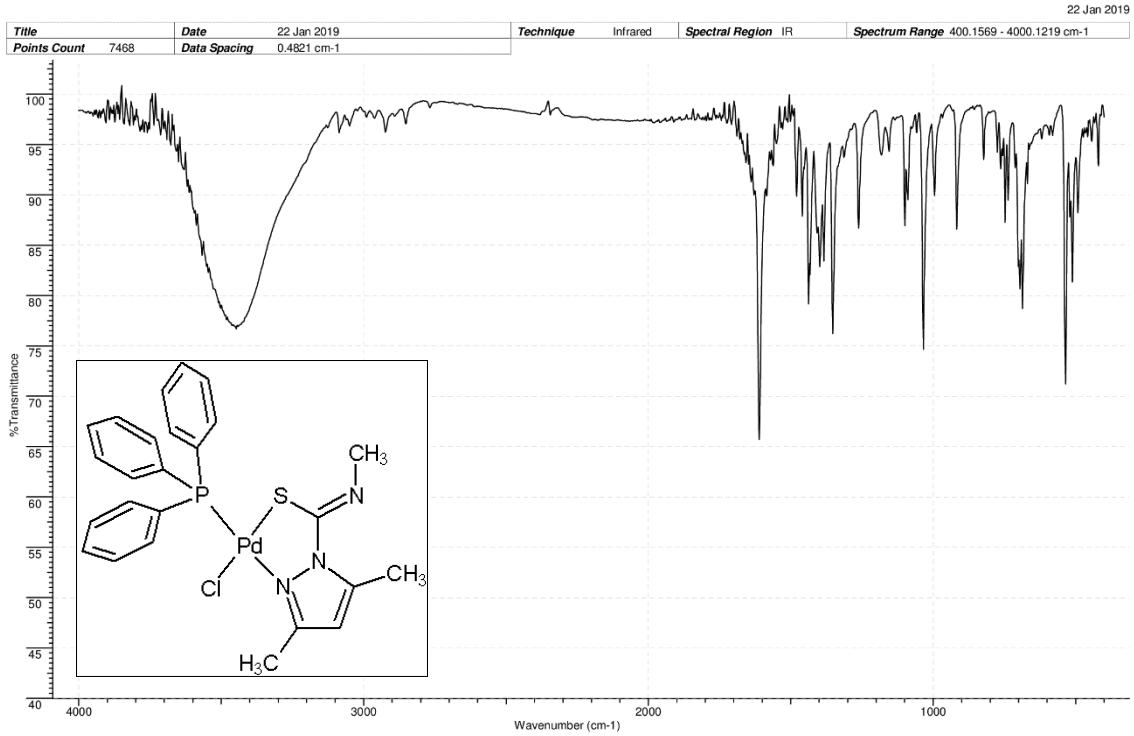

Fig. S42. Infrared spectra of complex **2**

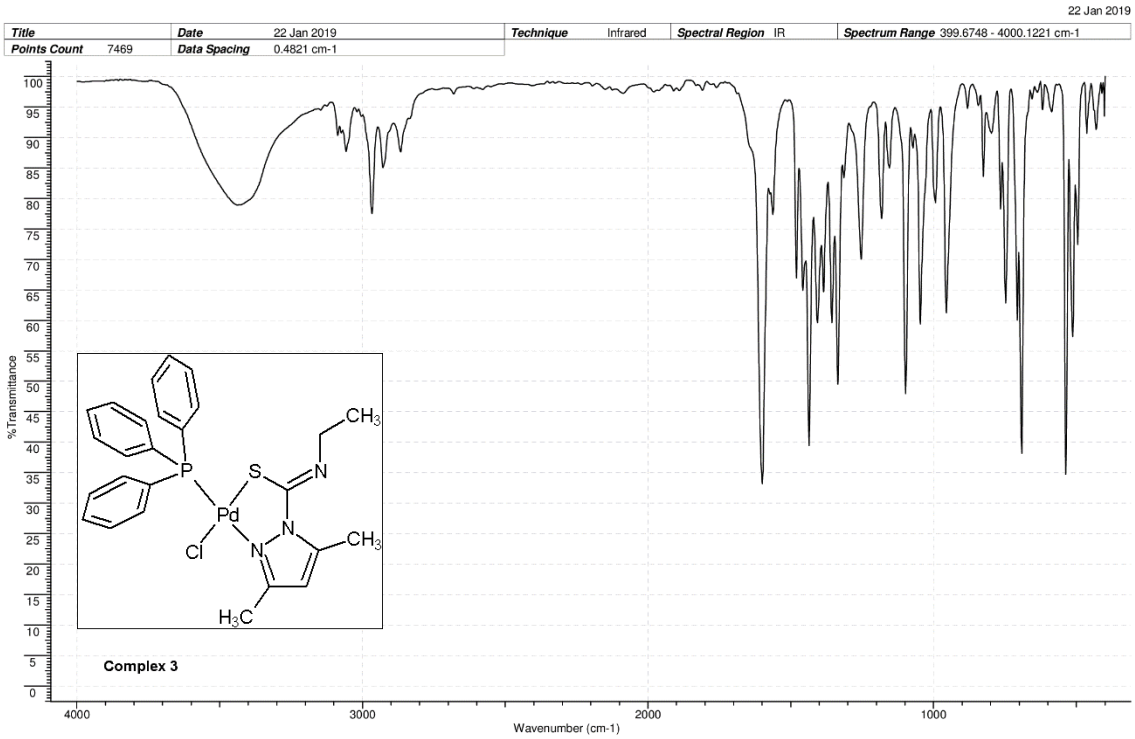

Fig. S43. Infrared spectra of complex **3**

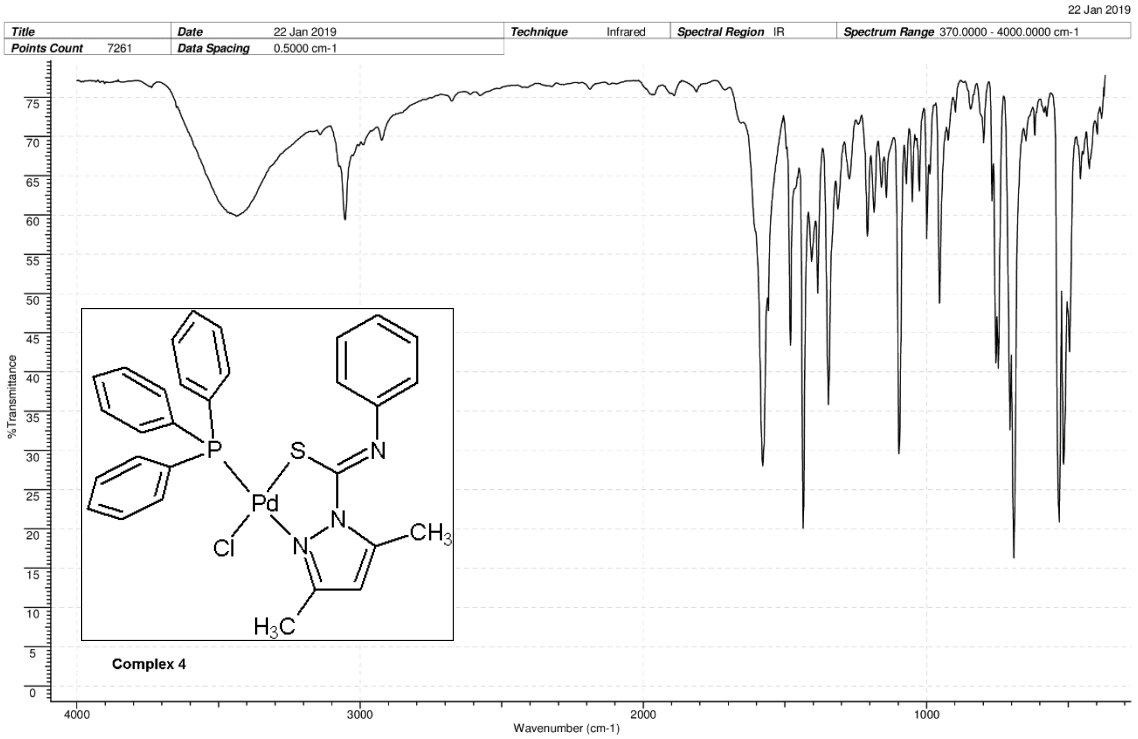

Fig. S44. Infrared spectra of complex **4**

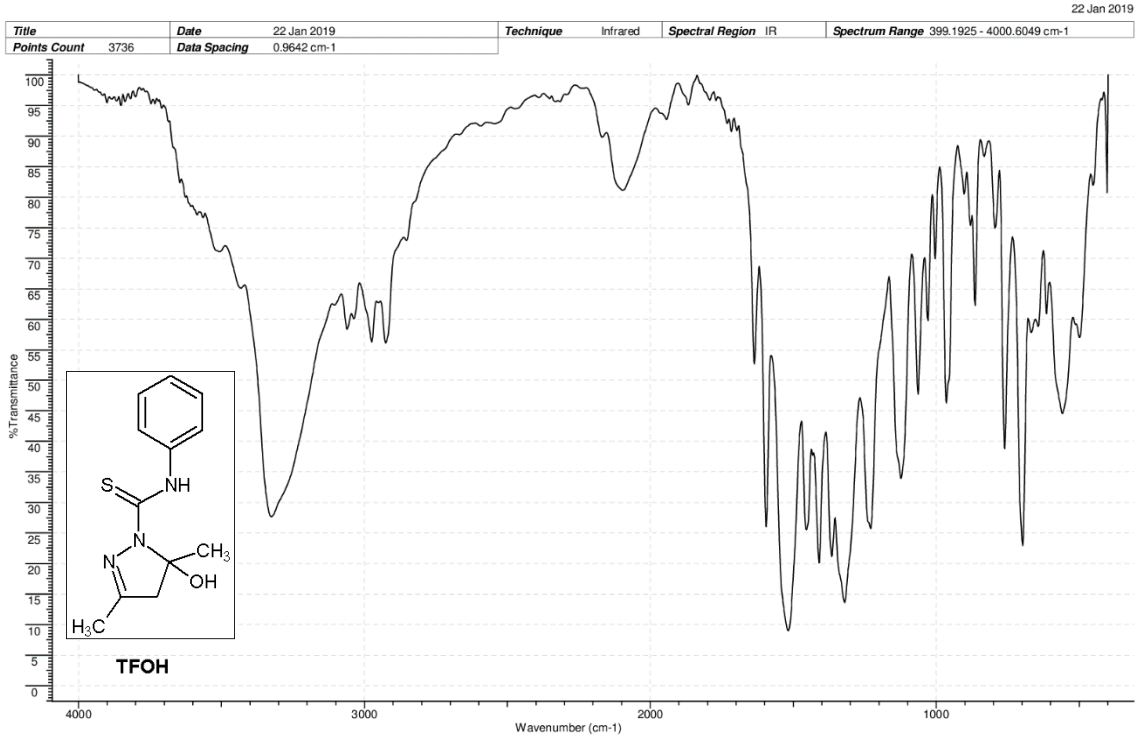

Fig. S45. Infrared spectra of compound **L_4'**

Table S4. Infrared Spectroscopic Data Assignments (in KBr) for synthetized N,S-ligands and complexes (wavenumbers, cm^{-1}).

L_1	1	L_2	2	L_3	3	L_4'	4	vibrational modes
						3250		**vOH**
3386								**vNH**
3240	3295	3328	-	3325	-	3325		**vNH**
3134	3074		3085		3086	3060		**vCH_{sp2}**
	3054		3049	-	3057	3036	3053	**vCH_{sp2}**
2990	2985	2976	2962	2975	2967	2974		**vCH_{sp3}**
2925	2923	2925	2923	2927	2928	2925	2923	**vCH_{sp3}**
			2852	2876	2867			**vCH_{sp3}**
			-	2584	-			**vSH**
1577	1436	1574	1437	1577	1436	1593	1435	**vCN_{ring}**
1599	2086	1523	1610	1516	1600	1513	1578	**vCN (thioamide I)**
	1481		1479		1480		1480	**vCC_{PPh3}**
1341	1353	1336	1352	1335	1335	1336	1346	**$vCC_{pyrazole}$**
1250	1273	1260	1262	1245	1253	1245	1273	**δCN + δCH + δNH**
	1096	-	1099	-	1098	-	1097	**q_{PPh3}**
1029	1051	1032	1034	1035	1046	1054	1050	**vNN_{ring}**
973		971	-	976	-	965		**vCS + δsNH**
880	920	936	916	961	955	883	954	**δrCH**
808	691	798	695	801	705	801	692	**vCS**
	746	-	747	-	748	-	746	**δCH_{PPh3}**
		-		-		698	755	**δCH_{Ph}**

S2.3. MS-ESI Spectroscopy

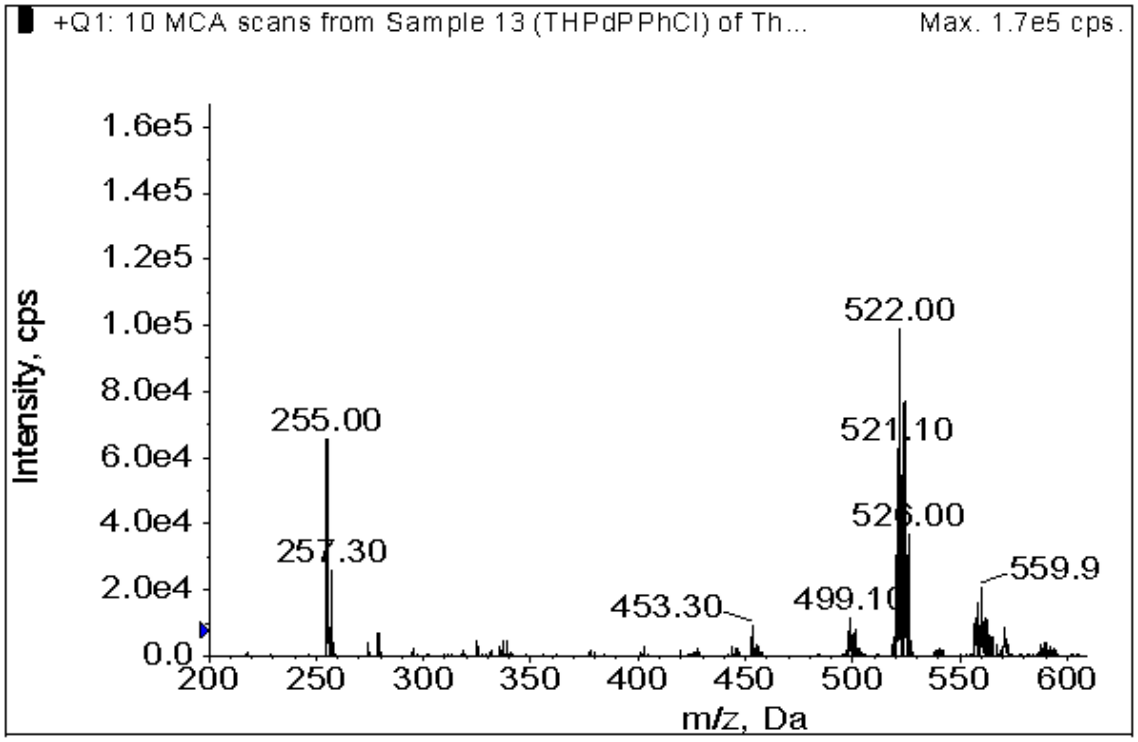

Fig. S46. Mass spectra of compound **1**

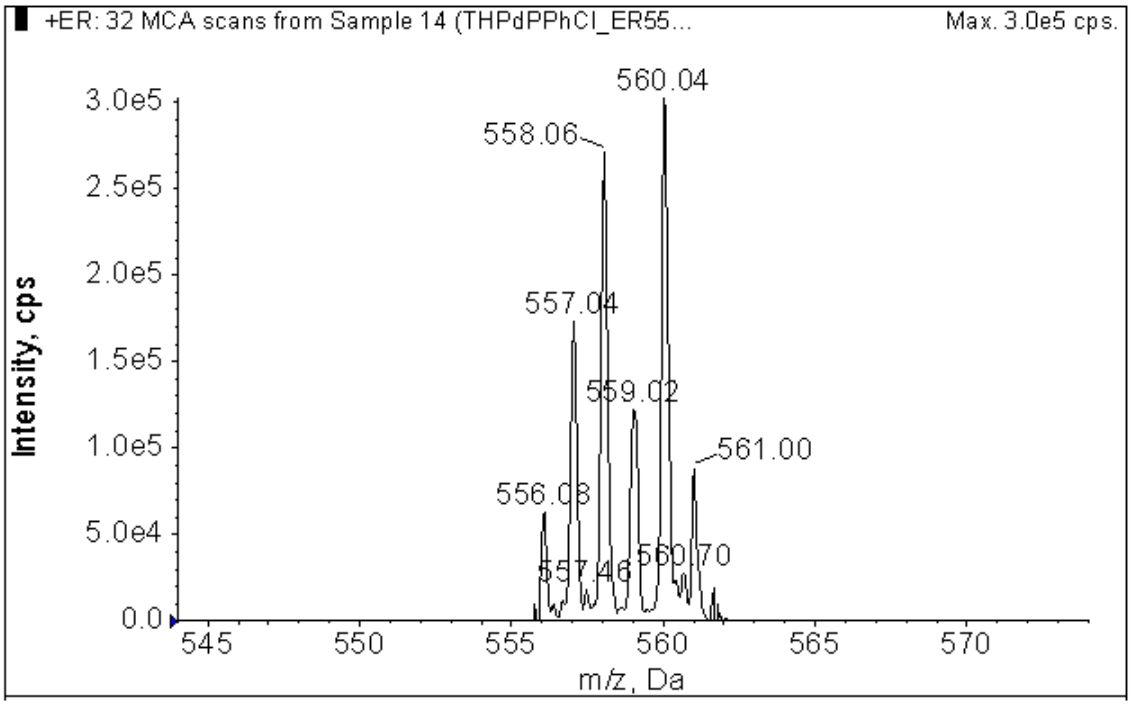

Fig. S47. Enhanced mass resolution spectra of compound **1**

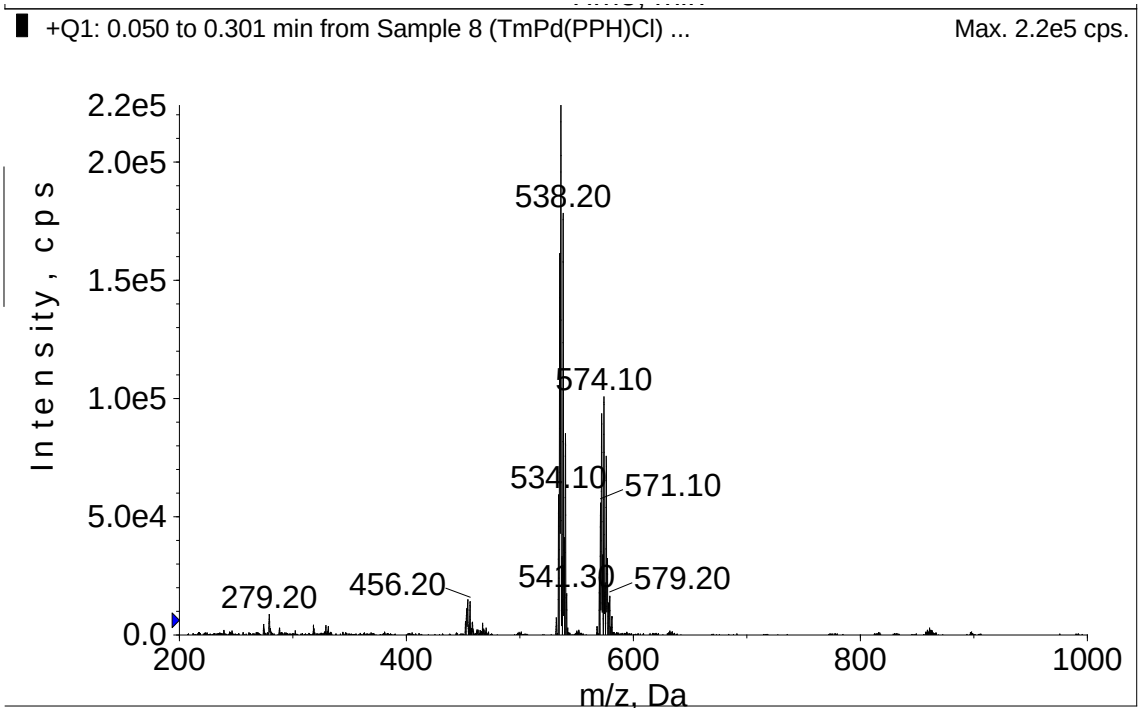

Fig. S48. Mass spectra of compound **2**

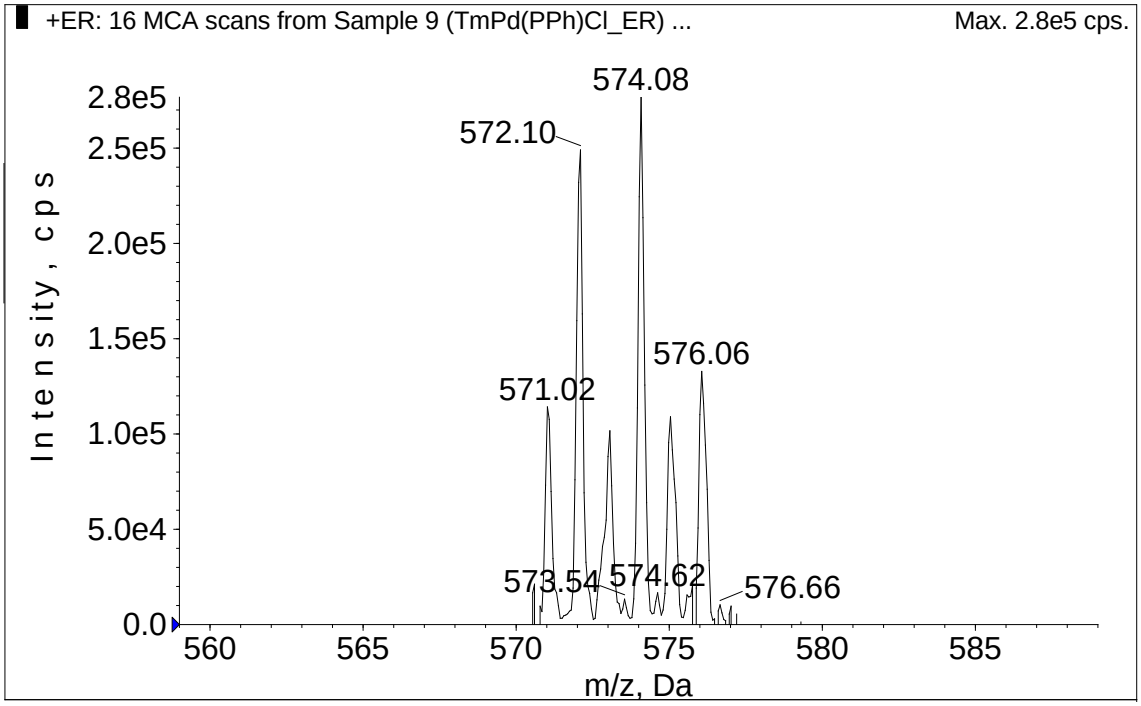

Fig. S49. Enhanced mass resolution spectra of compound **2**

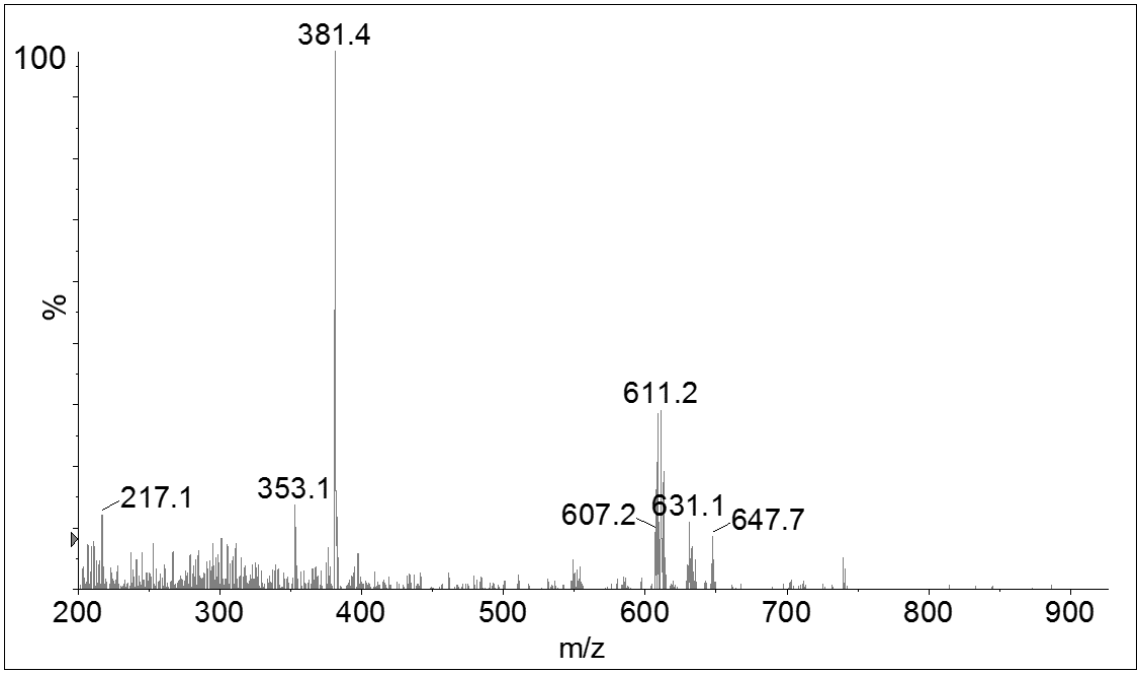

Fig. S50. Mass spectra of compound **3**

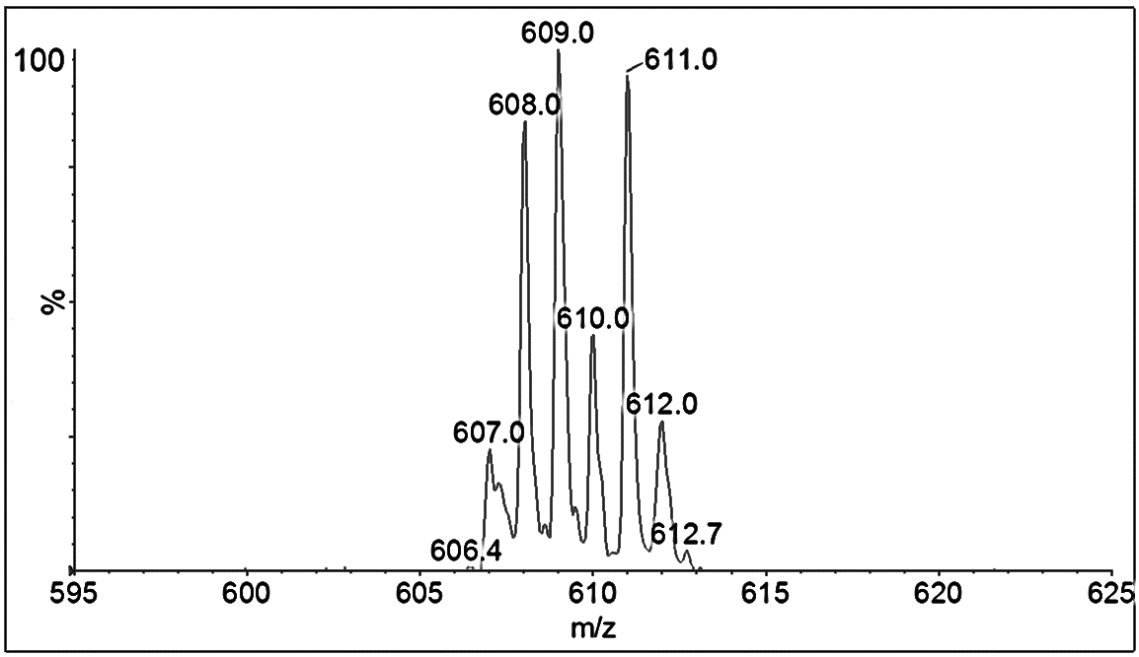

Fig. S51. Enhanced mass resolution spectra of compound **3**

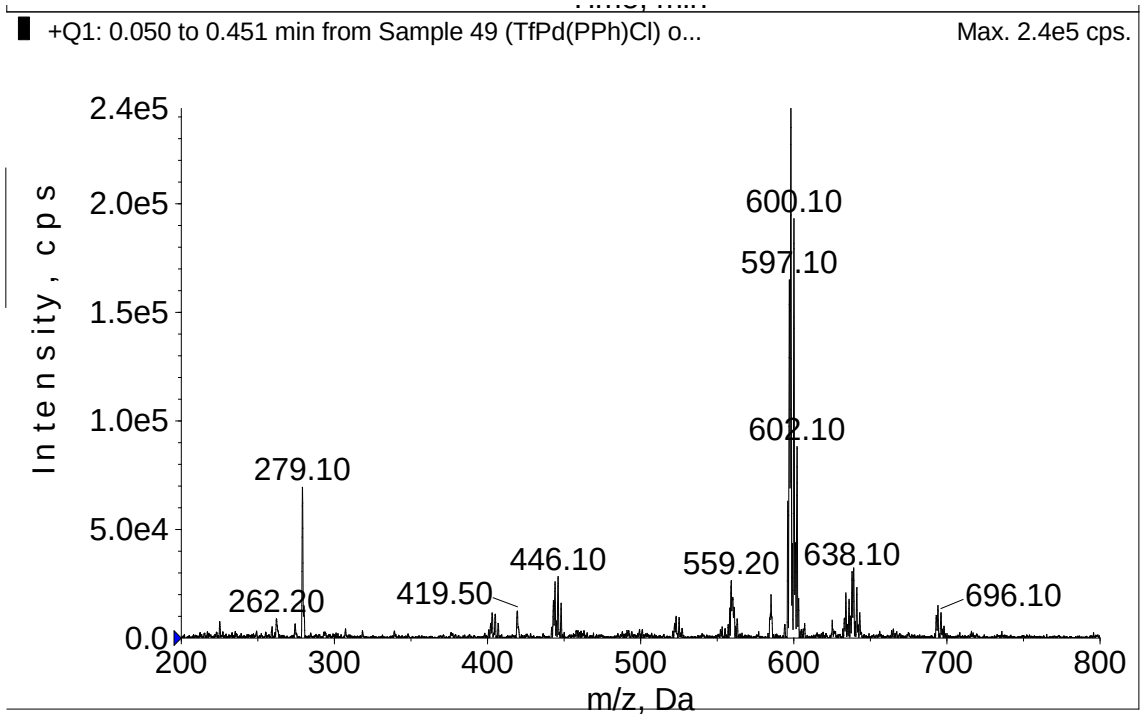

Fig. S52. Mass spectra of compound **4**

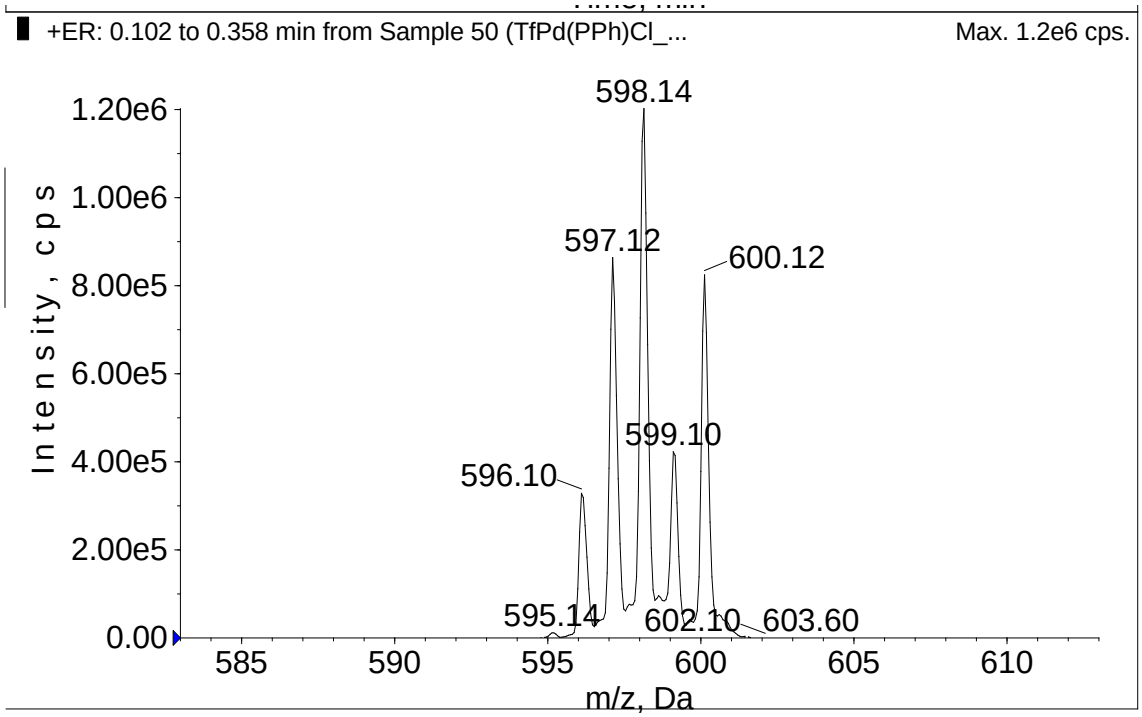

Fig. S53. Enhanced mass resolution spectra of compound **4**

S3. Biological activity data

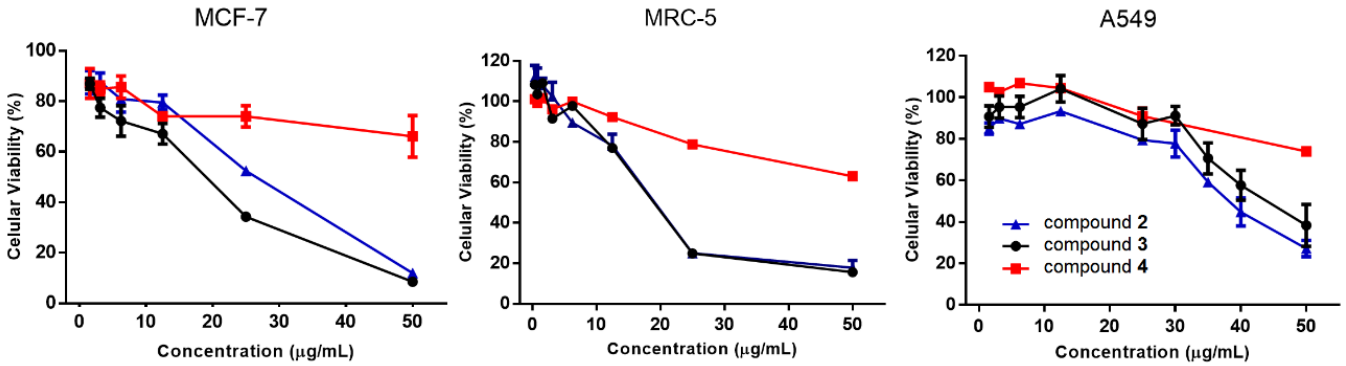

Fig. S54. Cell viability results after compound **2**-**4** treatment for 48 h.

Table S5. Activity of cathepsin L and B in presence of **2**-**4** in 10 and 100 μM.

Enzyme	Compound	IC_{50} (μM)	% of residual activity at 10 μM	% of residual activity at 100 μM
Cathepsin B	2	<100	75	31
	3	>10	91	Insoluble
	4	<10	42	Insoluble
Cathepsin L	2	<100	78	47
	3	>10	97	Insoluble
	4	<100	61	insoluble

References

1 G. M. Sheldrick, *Acta Cryst A,* 2008, **68**, 112-122.
2 G. H. Ribeiro, L. Colina-Vegas, J. C. T. Clavijo, J. Ellena, M. R. Cominetti and A. A. Batista, *Journal of Inorganic Biochemistry*, 2019, **193**, 70–83.
3 A. Wolfe, J. H. Shimer, T. Meehan, *Biochemistry*, 1987, **26**, 6392–6396.
4 A. I. Matesanz, E. Jimenez-Faraco, M. C. Ruiz, L. M. Balsa, C. Navarro-Ranninger, I. E. León and A. G. Quiroga, *Inorganic Chemistry Frontiers*, 2018, **5**(1), 73–83.
5 W. Villarreal, L. Colina-Vegas, G. Visbal, O Corona, R. S. Corrêa, J. Ellena, M. R. Cominetti and A. A. Batista, M. Navarro, *Inorganic Chemistry Frontiers*, 2017, **56**, 3781–3793.
6 J. Ruiz, C. Vicente, C. de Haro and D. Bautista, *Inorganic Chemistry*, 2013, **52**(2), 974–982.